Niche-specific genome degradation and convergent evolution shaping *Staphylococcus aureus* adaptation during severe infections

Stefano G. Giulieri[a,b,c], Romain Guérillot[a], Sebastian Duchene[a], Abderrahman Hachani[a], Diane Daniel[a,d], Torsten Seemann[d], Joshua S. Davis[e,f], Steve Y.C. Tong[f,g], Bernadette Young[h], Daniel J. Wilson[i], Timothy P. Stinear[a]*, Benjamin P. Howden[a,b,d]*

[a] *Department of Microbiology and Immunology, The University of Melbourne at the Doherty Institute for Infection and Immunity, Melbourne, Australia*

[b] *Department of Infectious Diseases, Austin Health, Heidelberg, Australia*

[c] *Victorian Infectious Diseases Service, Royal Melbourne Hospital, Melbourne, Australia*

[d] *Microbiological Diagnostic Unit Public Health Laboratory, The University of Melbourne at the Doherty Institute for Infection and Immunity, Melbourne, Australia*

[e] *Department of Infectious Diseases, John Hunter Hospital, Newcastle, New South Wales, Australia*

[f] *Menzies School of Health Research, Charles Darwin University, Casuarina, Northern Territory, Australia*

[g] *Victorian Infectious Disease Service, Royal Melbourne Hospital, and University of Melbourne at the Peter Doherty Institute for Infection and Immunity, Melbourne, Victoria, Australia*

[h] *Nuffield Department of medicine, Oxford*

[I] *Big Data Institute, Nuffield Department of Population Health, Li Ka Shing Centre for Health Information and Discovery, Old Road Campus, University of Oxford, Oxford*

OX3 7LF, UK

*Joint Senior author

#Address correspondence to Benjamin P. Howden, bhowden@unimelb.edu.au

Keywords: within-host evolution, adaptation, *Staphylococcus aureus*, genomics

ABSTRACT

During severe infections, *Staphylococcus aureus* moves from its colonising sites to blood and tissues, and is exposed to new selective pressures, thus potentially driving adaptive evolution. Previous studies have shown the key role of the *agr* locus in *S. aureus* pathoadaptation, however a more comprehensive characterisation of genetic signatures of bacterial adaptation may enable prediction of clinical outcomes and reveal new targets for treatment and prevention of these infections. Here, we measured adaptation using within-host evolution analysis of 2,590 *S. aureus* genomes from 396 independent episodes of infection. By capturing a comprehensive repertoire of single-nucleotide and structural genome variations, we found evidence of a distinctive evolutionary pattern within the infecting populations compared to colonising bacteria. These invasive strains had up to 20-fold enrichments for genome degradation signatures and displayed significantly convergent mutations in a distinctive set of genes, linked to antibiotic response and pathogenesis. In addition to *agr*-mediated adaptation we identified non-canonical, genome-wide significant loci including *sucA-sucB* and *stp1*. The prevalence of adaptive changes increased with infection extent, emphasising the clinical significance of these signatures. These

findings provide a high-resolution picture of the molecular changes when *S. aureus* transitions from colonisation to severe infection and may inform correlation of infection outcomes with adaptation signatures.

INTRODUCTION

While *Staphylococcus aureus* is one of the most important human pathogens (1), its common interaction with the human host is colonisation, usually of the anterior nares (2). Comparatively, severe, life-threatening infections such as bacteraemia or osteomyelitis occur very rarely. This suggests that at the macro-evolutionary level *S. aureus* is primarily adadpted to its natural ecological niche (the nasal cavity) and to specific selective pressures arising in this environment, such as competition with the resident microbiota (3). By contrast, during invasive infection, a new fitness trade-off needs to be achieved to adjust to environmental challenges that include innate and acquired immune responses (4), high-dose antibiotics (5) and nutrient starvation (6). These trade-offs could occur across three potentially distinctive dynamics of micro-evolution during colonisation and infection (within the colonising population, from colonising to invasive and within the invasive population), leading to nose-adapted, early infection-adapted and late infection-adapted strains. Identifying infection-adapted strains might assist precision medicine strategies for infection prevention and management, and refine the understanding of *S. aureus* pathogenesis versatility, as mutational footprints of selection mirror functions that are critically important for bacterial survival during invasion.

Emerging genomic approaches for analysis of within-host evolution are among the most powerful means to study bacterial host adaptation (7-9). Studies have shown

the remarkable diversity and evolution of colonising populations of *Streptococcus pneumoniae* (10) and *S. aureus* (11). In *S. aureus* and *Enterococcus faecium* it has been shown that transition from colonisation to invasion favours strains with specific adaptive signatures (12, 13), while evidence of niche adaptation was noted in a within-host study of bacterial meningitis due to *S. pneumoniae* (14). Further, phenotypic and genomic adaptation (often in response to antibiotic pressure) has been investigated during selected episodes of persistent invasive infections due to *S. aureus* (15-17), *Pseudomonas aeruginosa* (18), *Salmonella enterica* (19), and *Mycobacterium tuberculosis* (20). To increase power, bacterial within-host evolution studies have leveraged on large collections of paired samples coupled with statistical models of genome-wide mutation rates (7, 14, 21) and extended the analysis to include chromosomal structural variation (17, 22, 23) as well as intergenic mutations (22, 24).

Convergent evolution among separated (independent) episode of colonisation or infection is a key indication of adaptation in evolution analyses. However, with the notable exception of one study of cystic fibrosis (25), the convergence has generally been weak in within-host studies of *S. aureus* infections, with no convergence at all (17) or significant enrichment limited to the *S. aureus* master regulator *agr* (12). We hypothesised that in addition to the small sample size, the extended range of bacterial functions potentially under selective pressure (each function being potentially targeted by diverse patho-adaptive mutations) has hampered the identification of important adaptation mechanisms. To overcome the limitations of studies to date, we have pooled all publicly available *S. aureus* within-host evolution studies, and complemented this with a new dataset from a recent *S. aureus* clinical

trial (26), in a single large-scale analysis. Rather than focussing on point mutations and small insertions/deletions alone, we leveraged multiple layers of genome annotation (encompassing coding regions, operons, intergenic regions and functional categories) and included chromosome structural variants to compile a comprehensive catalogue of bacterial genetic variation arising during host infection. This strategy enabled the detection of convergent adaptation patterns at an unprecedented resolution. We also outline distinctive signatures of adaptation during colonisation, upon transition from colonisation to infection and during invasive infection.

RESULTS

The *S. aureus* within-host evolution analysis framework.

We compiled a collection of 2,251 *S. aureus* genomes from 267 independent episodes of colonisation and/or infection, reported in 24 genomic studies (12, 17, 23, 27-47) (Table S1). We supplemented this dataset of publicly available sequences with unpublished sequences from 603 serial invasive isolates collected within the CAMERA-2 trial (26).

After excluding sequences failing quality control and genetically unrelated strains within the same episode, 2,590 genomes (1,397 invasive, 1,193 colonising) from 396 episodes were included in our within-host evolution analysis (Figure 1, Table 1, Supplementary files 1 and 2). The most prevalent lineages in the collection were sequence type (ST) 30 (342 strains, 13%), ST 22 (277 strains, 11%) and ST 5 (271 strains, 11%); 1001 strains (39%) were *mecA* positive. The collection was representative of the global *S. aureus* diversity, with an even distribution of colonising and invasive strains across the major clades (Figure 2A). The most

125 frequent infection syndrome was bacteraemia without focus (152 episodes, 38.4%),
126 while nasal carriage (166 episodes, 42%) was the most prevalent colonisation
127 condition (Table 1).
128
129
130 Our within-host evolution analysis strategy identified 4,556 genetic variants (median
131 3 per episode, range 0-237) (Supplementary file 3). Importantly, by investigating both
132 point mutations and structural variation, we were able to uncover 214 large deletions
133 (≥ 500 bp), 160 new insertion sequences (IS) insertions and 609 copy number
134 variants, underscoring the role of large chromosome structural variation in within-
135 host evolution. To increase the evolutionary convergence signal by aggregating
136 mutations in functionally consistent categories, we annotated all genetic variants
137 using multiple datasets, including coding sequences, regulatory intergenic regions,
138 operons and gene ontologies (Figure 1C).
139
140 **Distinctive evolutionary patterns define nose-adapted, early infection-adapted**
141 **and late infection-adapted strains**
142 Based on the working hypothesis that *S. aureus* host adaptation patterns differ
143 according to whether the strains are nose-colonising, collected at an early stage of
144 infection or at a late infection stage (i.e associated with persistence or treatment
145 failure), we assessed whether it was possible to define i) general paradigms of
146 genetic variation and ii) specific convergence signatures. Thus, we classified within-
147 host acquired variants into three groups according to their most likely location in the
148 within-host phylogeny: (i) between colonising strains (type C>C); (ii) between
149 colonising and early infection adapted strains (type C>I); and (iii) between invasive

150 strains (type I>I). Overall, the 396 infection episodes included in the analysis allowed
151 us to independently assess 166 type C>C, 118 type C>I and 312 type I>I within-host
152 variants. In 95 cases there were sufficient samples to assess all 3 types within the
153 same episode (Figure 2A).
154 We have previously shown that invasive strains from persistent or relapsing
155 infections exhibit a high proportion of protein-truncating mutations (17). A similar
156 enrichment of protein-truncating variants was identified within invasive strains as
157 compared to strains from asymptomatically colonised individuals (12, 27). We
158 reasoned that if this indicates genome degradation during infection, infecting strains
159 might also be enriched for other loss-of-function mutations caused by structural
160 variants, such as movement of insertion sequences (48) and large deletions, leading
161 to complete or partial gene loss (49). In addition, we hypothesised that mutations
162 and IS insertions in intergenic regions might contribute to altering gene expression or
163 activity by interfering with the expression of key genes or operons (50).
164
165 Therefore, we calculated the prevalence of intergenic mutations, protein-truncating
166 mutations, IS insertions and large deletions among all variants and compared it
167 between type C>C (colonising-colonising), type C>I (colonising-invasive) and type
168 I>I (invasive-invasive) variants. Strikingly, the distribution of mutations according to
169 the predicted effect differed substantially in invasive-invasive pairs when compared
170 to mutations identified between nose-colonising and invasive strains and within
171 colonising strains (Figure 2 and Table 2). As compared to type C>C variants,
172 variants emerging within the infecting strains were enriched for intergenic mutations
173 (neutrality index [NI] 2.5; $p = 1.8 \times 10^{-16}$) and protein-truncating mutations (NI 2.4; p =

174 4.8 x 10^{-10}). In contrast, no significant enrichment was observed among type C>I
175 variants.
176
177 While large deletions were significantly more enriched in type I>I variants (NI 4.0, p =
178 1.1 x 10^{-15}), the strongest evidence for enrichment (NI 19.9, p = 1.6 x 10^{-42}) was
179 found for IS insertions. We and others have previously shown that new insertions of
180 IS*256* may provide an efficient mechanism of genomic plasticity in invasive *S.*
181 *aureus* strains (17, 39, 50). Here, we expand this observation in a larger dataset and
182 show that this mechanism is not limited to IS*256* (Figure 2 – figure supplement 2). As
183 shown in Figure 2, two invasive strains exhibited a burst of > 10 new IS insertions
184 (IS*3* and IS*256*, respectively). It has been shown that IS activation occurs under
185 stress conditions, such as antibiotic exposure and oxidative stress (51), which is
186 consistent with the selection environment encountered by invasive strains. However,
187 these bursts occurred only in 2/1,068 adapted invasive strains.
188
189 Overall, these data support a model, where late infection-adapted strains show an
190 enrichment for variants that are predicted to exert a stronger functional impact, either
191 by producing a truncated protein or by potentially interfering with intergenic
192 regulatory regions, through point mutations or IS insertions. This strong genome
193 degradation signature appears to be specific to type I>I variants and was absent in
194 type C>I variants, suggesting that the bottleneck effect upon blood or tissue invasion
195 doesn't explain it. To assess whether this general enrichment of non-silent evolution
196 represented a signature of positive selection or derived from within-host gene
197 obsolescence occurring during invasive infection, we further investigated signals of

gene, operon and pathway specific enrichment across independent episodes of infection.

Gene enrichment analysis identifies significant hotspots of adaptation.

To identify signatures of adaptation, we first counted how many times each coding sequence was mutated independently across distinct colonisation/infection episodes (Figure 3, Tables 3 and Table 3 – table supplement 1, Supplementary file 3). We considered all protein-modifying mutations either predicted to cause a gain or loss of function to the locus: non-synonymous substitutions, truncations, IS insertions or deletions. To ensure consistency across the dataset, we retricted our analysis to genes with a homologue in reference strain FPR3757 (excluding plasmid genes and phage genes). Mutations were considered independent if they arose in distinct colonisation/infection episodes. To assess whether the convergent signals were a reliable indication of adaptation, we applied a gene enrichment analysis for protein-altering mutations which computes a length-corrected gene-level enrichment of protein-modifying mutations and estimates the significance of the enrichment for each gene using Poisson regression (12).

When applying a Bonferroni-corrected significance threshold ($4.6x10^{-5}$), mutations in *agrA* were highly significantly enriched across the entire dataset (45 fold enrichment, $p=7.0x10^{-28}$). Other significantly enriched genes were *agrC* (13 fold enrichment, $p=2.8x10^{-10}$), *stp1* (14 fold enrichment, $p=1.1x10^{-7}$) and *mprF* (6 fold enrichment, $p=4.6x10^{-6}$). The gene *sucA* reached near-significance (5 fold enrichment, $p=6.8x10^{-5}$). Mutations in genes most significantly targeted by convergent evolution were evenly distributed across the *S. aureus* phylogeny, indicating that these adaptative

mechanisms were not specific to selected lineages (Figure 3 – figure supplement 1). Using dN/dS analysis, we confirmed signatures of positive selection in the most significantly enriched genes, although only *agrA* reached statistical significance (Figure 3 – figure supplement 2 and supplementary file 4).

We found that several genes with the most significant enrichment (*agrA*, *agrC, stp1*, *sucA*) were recurrently mutated across all three within-host evolutionary scenarios, implying a global role in *S. aureus* adaptation during colonisation and invasion. This suggests partial adaptation of *S. aureus* strains upon invasion. It has been previously shown that adaptive mutations, particularly within the quorum sensing accessory gene regulator (*agr*), are enriched in invasive *S. aureus* strains, suggesting that adapted strains are more prone to be involved in invasive disease (12, 27, 47, 52). While the key role of *agr* was consistent with previous evidence from clinical and experimental studies, the high number of recurrent *sucA* mutations was suprising. This metabolic gene encodes for the α-ketoglutarate dehydrogenase of the tricarboxylic acid cycle, and recent work has revealed the functional basis of its potential role in adaptation. Its inactivation was found to lead to a persister phenotypye (53) and *sucA* was a hotspot of metabolic adaptation to antibiotics in a recent *in vitro* evolution study (54).

To confirm that our gene enrichment analysis (focused on point mutations and IS insertions and limited to genes with FPR3757 homologs) captured the large part of adaptation, we analysed variation due to large deletions and copy number variation, which were not included in the gene enrichment analysis. We observed multiple independent deletions and amplifications mainly in phage genes (Figure 3 – figure

supplement 3 and Figure 3 – figure supplement 4). We also repeated the gene enrichment analysis with all mutated genes (with and without FPR3757 homologs) and found very similar results, with only two hypothetical proteins with no FPR3757 homolog among the genes with most significant enrichment (Figure 3 – figure supplement 5).

Combining multiple mechanisms of adaptation and multilayered annotation increases the signal of convergent evolution

To increase our ability to capture signatures of adaptation from convergent evolution, we extended our analysis beyond coding sequences, to integrate the genetic variation signals issued from intergenic mutations and IS insertions in intergenic regiions. This multi-layered annotation of mutated regions was shown to increase the amount of information gained from *in vitro* adaptive evolution experiments (55). Such methodology allows for an advanced classification of intergenic mutations based on regulatory sequences including promoters and transcription units based on data acquired from RNAseq experiments (56, 57).

Using this approach, we were able to assign 150/1237 (11%) of all intergenic mutations and IS insertions to a predicted regulatory region. We found that the *agr*, *sucAB*, *walKR* operons had the strongest convergent evolution signal with 28, 13 and 13 independent mutations (Supplementary file 5). Mutations within these loci were significantly (*agr*, 12-fold enrichment, p=1.1e-21; *sucAB*, 4-fold enrichment, p=4.5e-5) or near-significantly enriched (*walKR*, 3-fold enrichment, p=1.7e-4) (Figure 4). Interestingly, promoter mutations represented 2/13 (15%) of the *walKR* operon mutations, indicating that potentially impactful intergenic variants may be missed

when considering only coding regions. Further, new IS insertions were found within type I>I (invasive-invasive) variants: three insertions into *agrC* (predicted to inactivate the gene, as shown previously in staphylococci (58, 59)) and an insertion 159 bp upstream of *walR*, in a region encompassing its cognate promoter. Together with the strong enrichment for IS insertions within type I>I variants, the location of these insertions in recurrently mutated operons suggests that IS insertions contribute to the adaptive evolution of *S. aureus* during invasive infection.

Adaptation within the invasive population is distinctive and strongly driven by antibiotics.

The excess of non-silent evolution (and potentially function-altering) within invasive strains suggested that strong, specific selection pressure occurs within the invasive populations (type I>I variants). We therefore assessed genes that appeared to be specifically mutated or inactivated during infection. We performed our gene- and operon-enrichment analysis for each type of within-host variants separately (i.e within the colonising population, between colonising and invasive strains and within the invasive population) (Figure 5).). We found that *agrA* mutations were highly enriched in any group of variants, and particularly prevalent between colonising and invasive strains (type C>I variants), consistent with a previous study that is included in this analysis (12). Among type I>I variants (between invasive strains), a significant enrichment was observed in *mprF* (18 fold enrichment, $p = 2.8 \times 10^{-9}$), *agrC* (24 fold enrichment, $p=2.1 \times 10^{-7}$), *rpoB* (10 fold enrichment, $p = 8.8 \times 10^{-6}$). Other genes that were strongly enriched in type I>I variants (below the Bonferroni-corrected threshold, but above the suggestive significance threshold, Figure 5), included *walR* (22 fold enrichment, $p = 3.5 \times 10^{-4}$), *stp1* (20 fold enrichment, $p=4.2 \times 10^{-4}$), *yjbH* (19 fold

298 enrichment, p = $5.4x10^{-4}$), *sgtB* (19 fold enrichment, p=$5.5x10^{-4}$) and *purR* (18 fold
299 enrichment, p = $5.8x10^{-4}$).
300
301 The enrichment for mutations in *mprF, rpoB, stp1, sgtB* and in the *walKR/yycH*
302 operon (11 fold enrichment, p = $9x10^{-9}$, see Figure 5 – figure supplement 1 for the
303 operon enrichment analysis) highlights the role of antibiotic pressure in shaping
304 adaptation within the invasive population, since these loci are hotspots of adaptation
305 to key anti-staphyloccal antibiotics that are often used in invasive infections
306 (rifampicin, daptomycin, vancomycin). For example, the essential two-component
307 regulator *walKR/yycFG* (and its associated genes *walH*/*yycH)* have been shown to
308 have a key role in vancomycin resistance in one of the within-host evolution studies
309 included in this analysis (41), while mutations in both *stp1* and *sgtB* have been
310 observed in vancomycin-adapted strains (60).
311
312 Notably, the most significant gene signatures in invasive strains might have been
313 selected in response to other selective pressures, including the host immune
314 response during infection. For example, *rpoB* mutations have been associated with
315 pleiotropic effects, including co-resistance to vancomycin, daptomycin and oxacillin
316 and immune evasion, suggesting a potential role in adaptation beyond the response
317 to the selective pressure from rifampicin (61). This hypothesis is supported by the
318 presence of mutations (such as the *rpoB* R503H substitution and N405 inframe
319 deletion) outside the rifampicin-resistance determining region
320
321 Pleiotropic phenotypes are also likely to underlie the enrichment of *yjbH* with
322 invasive strains, which was mutated four times (of which three were truncations), yet

only one mutations was found in colonising strains or early infection-adapted strains. This gene has a cysteine-rich domain that is homologous to *dsbA* in *E. coli*. One of its roles in *S. aureus* is to facilitate the ClpXP-dependent degradation of the transcriptional regulator Spx (62). Inactivation of *yjbH* has been associated with oxacillin (63) and vancomyin (64) resistance, impaired growth (65) and reduced virulence in animal models (66), indicating that *yjbH* mutations may influence both host-pathogen interaction and antibiotic resistance. Finally *purR*, a purine biosynthesis repressor, has been recently characterised beyond its metabolic function: interestingly it was shown to be a virulence regulator (67), where *purR* mutants displayed higher bacterial counts following mice infection, increased biofilm formation (68) and higher capacity to invade epithelial cells (69).

We perfomed a gene set enrichment analysis (GSEA), using gene ontology and antibiotic resistance gene annotations (70). The GSEA, stratified by variant type, showed significant enrichment only in type I>I (invasive-invasive) variants, further underscoring the higher level of adaptation in this group (Figure 5 – figure supplement 2 and supplementary file 6) and confirmed the broad functional implications of the most enriched genes and operons with the invasive populations, since among the ontologies that were significantly enriched within the invasive population, we found the categories "DNA binding" (normalised enrichment score [NES] = 1.6, false-discovery rate (FDR)-ajusted p = $9x10^{-4}$), "pathogenesis" (NES = 1.7, ajusted p = $4x10^{-3}$) and "antibiotic response" (NES = 1.8, adjusted p = 7×10^{-3}).

Taken together, these findings point to six key genetic loci that appear to have an important role in *S. aureus* adaptation during during invasive infections. These loci

348 are associated with either antibiotic resistance (*mprF*, *rpoB*, *stp1*, *sgtB*, *walKR*),
349 pathogenesis (*agrAC*, *purR*) or both (*yjbH*).
350
351 **A mutations co-occurrence network defines loci under within-host co-**
352 **evolutionary pressure**
353 Epistasis, defined as the interaction of multiple mutations on a given phenotype (71),
354 plays a role in adaptive evolution in bacteria, particularly in antibiotic resistance (72-
355 74). Whether epistatic interactions could promote *S. aureus* adaptation during
356 infection remains unknown. Indentifying these interactions would enable
357 identification of combinations of mutations underlying bacterial adaption during
358 infection and refine the prediction of infection outcomes. Here, we assessed co-
359 occurrence of mutations and mutated genes across independent episodes of
360 colonisation/infection. While co-occurrence may simply result from co-selection (e.g.
361 simultaneous exposure to two different antibiotics), it may also indicate putative
362 epistatic interactions, that could be explored in terms of potential impact on adaptive
363 phenotypes (75).
364
365 First, we explored co-occurrence of mutations, and found only one case where the
366 same mutations co-occurred in more than one independent episode. The two
367 mutations were an inframe deletion within hypothetical protein SAUSA300_2068 and
368 a A60D substitution of the gene *ywlC*. These genes are closely located in FPR3757.
369 While the co-occurrence could be explained by recombination, recombination is
370 expected to be rare amongst within-host *S. aureus* populations in general (43) and
371 even rarer within invasive strains. YwlC is a threonylcarbamoyl-AMP synthase *in E.*
372 *coli*, thus it is possible that SAUSA300_2068 is also a ribosomal protein. Ribosomal

373 proteins can display regulatory activity (76), and could plausibly be targets of
374 adaptation to both antibiotics and the host/intracellular survival. This specific case of
375 convergent co-occurrence of mutations was detected within type I>I variants.
376
377 When assessing interactions at gene level (i.e. co-occurrence of the same altered
378 protein sequences across independent episodes), we found the strongest interaction
379 between the *agrA* and *agrC* genes (Figure 6). While this is consistent with the high
380 convergence of mutations in the *agr* locus, this suggests that strains acquire multiple
381 mutations within the locus, possibly further impacting *agr* activity. Interestingly, no
382 convergent co-occurrence signature compatible with possible epistasis was
383 observed within the *walKR* locus, the other operon with a high number of
384 independent mutations; which could be due to the essentiality of *walKR* in *S. aureus*
385 (77). Collectively, *agr* locus mutations interacted with 17 other mutated genes, the
386 strongest interaction being with *stp1*. Since *stp1* (a serine/threonine phosphatase)
387 has been previously associated with virulence regulation (78), this interaction
388 potentially indicates another mechanism by which adapted strains fine-tune the gene
389 expression profile that is already altered by *agr* mutations.
390
391 Another moderately strong interaction was observed between *rpoB* and *parC*, which
392 were co-mutated in three independent episodes. Given the association of *parC*
393 mutations with fluoroquinolone resistance (79), this interaction is likely to be an
394 example of co-selection due to co-exposure to fluoroquinolones and rifampicin.
395

396 **Clinical correlates of adaptive signatures within colonising and invasive**
397 **populations**

398 Genetic signatures of bacterial adaptation have been associated with infection
399 extent, for example enabling the prediction of extraintestinal infection with
400 *Salmonella enterica* (80). We have previously shown that adaptive mutations are
401 enriched in invasive infections, however, it is unclear whether bacterial adaptation is
402 more likely to be associated with distinctive clinical syndromes. To identify clinical
403 correlates of adaptive signatures we classified colonisation and infection episodes
404 based on the sites of collection and on clinical data obtained from the publications
405 (table 1 and Figure 7 – figure supplement 1). We then used the Jaccard index and
406 network analysis to compute node centrality as a global measure of adaptation for
407 each independent episode. The Jaccard index can be used as a simple marker of
408 the proportion of shared mutated genes between pairs of colonisation or infection
409 episodes (81). Node centrality allows to similtuaneously take into account the
410 strength of similarity between independent episodes (Jaccard index) and the number
411 of pairs with shared mutated genes (number of connections). Here, we limited the
412 analysis to the 20 most significantly enriched genes with each type of variant.
413
414 Our network analysis showed that adaptation was present in only a minority of
415 episodes within each type of variant (Figure 7 – figure supplement 2). With a
416 definition of adaptation based on a centrality value of more than 0, we found that the
417 proportion of adaptive episodes was 43%, 20% , 22% with type C>C, C>I and I>I
418 variants, respectively. In addition certain clinical syndromes were more strongly
419 associated with adaptation. Within the colonising population (type C>C variants),
420 almost 80% of cystic fibrosis episodes were adaptive, as opposed to one third of

episodes of skin colonisation in atopic dermatitis (Figure 7AB). This is consistent with within-host evolution studies showing strong convergent evolution signals among bacterial populations colonising individuals with cystic fibrosis, not only in case of *S. aureus* colonisation (25), but also *Pseudomonas aeruginosa* (7) and *Mycobacterium abscessus* (82), however, one study found adaptive evolution signals in atopic dermatitis (83). We also observed that adaptation among infection episodes correlated with infection extent. Episodes of infective endocarditis episodes displayed higher adaptation metrics (46% with centrality > 0) than bacteraemia with additional infection foci (28%) and bacteraemia without focus (17%) (Figure 7 D-E).

To explore the syndrome-specificity of adaptation signatures, we mapped mutations in the most significantly enriched adaptive genes to clinical syndromes of colonisation and infection (Figure 7 panels C and F). As expected, syndromes with high prevalence of adaptation had higher numbers of episodes with adaptive mutations; however, some genes appeared to be preferentially mutated. For example, *rpsJ*, *stp1* and SAUSA300_1230 were over-represented in cystic fibrosis, while no clear pattern of mutations was discernible for nasal carriage episodes. Within infection syndromes, *mprF* and *purR* mutations were more prevalent in endocarditis, and *yjbH* mutations were only found in severe infections (bacteraemias with additional foci and endocarditis). Some genes appeared to be distinctive for low adaptation groups (atopic dermatitis, skin infections), however the low number of adaptative mutations prevented an accurate assessment of these profiles.

DISCUSSION

Within-host evolution of bacterial pathogens such as *S. aureus* is thought to be governed by a combination of positive selection for variants that confers an advantage within the host, and fixation of mutations owing to genetic drift and relaxation of purifying selection (19, 84). Sudden changes in the effective population size (bottlenecks) can cause genetic drift, for example when a a single or few bacterial cells invade the bloostream or when a secondary infection foci is established in tissues and organs. Consistent with this view, animal studies have shown that after infecting the blood with a polyclonal population, bacteraemic infection is established stochastically by a single clone (85, 86). On the other hand, several lines of evidence support the role of positive selection and adaptive evolution during *S. aureus* infection. First, adaptive phenotypic features appear to be acquired during infection. The most obvious adaptative phenotype is secondary resistance to anti-staphylococcal antibiotics such as rifampicin, vancomycin (16), daptomycin (87), oxacillin (15). Crucially, these resistance phenotypes can be associated with pleiotropic, patho-adaptative phenotypes such as small colony variant and immune evasion (61, 88, 89). Further, phenotypic adaptation (e.g. loss of toxicity) has been observed upon transition from colonisation to infection (90), supporting the concept that invasive infection is linked to patho-adapted strains. At the molecular level, an excess of protein-truncating mutations in invasive strains (17) and in late colonising strains leading to infection (27) have been noted. While this observation alone could be explained by relaxed constraint resulting from reduced population size (84), it has been suggested that loss of gene function might be a common adaptation mechanism of within-host evolution (21), as supported by evidence of gene- or

468 pathway-specific enrichment of mutations across independent infection episodes
469 (12).
470
471 Despite support for adaptive evolution from previous studies, it has been difficult to
472 identify specific molecular signatures of adaptation during infection, due to the limited
473 power of previous within-host studies of bacteraemia and other serious *S. aureus*
474 infections, that were often limited to a restricted number of episodes. To increase our
475 ability to identify signatures of adaptation and find significantly enriched loci, we
476 analysed multiple sources of genetic variation (point mutations, large deletions, IS
477 insertions, copy number variants) in a large collection of independent episodes of *S.*
478 *aureus* colonisation and infection from 25 studies. We predicted that the main
479 advantage of our approach would be to increase the ability of detecting convergence
480 of genetic variants arising during invasive infections as opposed to those detected
481 during the colonisation and upon transition from colonisation to infection. To test this
482 hypothesis, we classified within-host variants based on their likely position in the
483 within-host phylogeny (Figure 1D).
484
485 Bacterial adaptation is promoted by genomic plasticity, however, within-host
486 evolution is characterised by low genetic variation (17). Based on our previous
487 genomic studies of *S. aureus* bacteraemia, we reasoned that chromosome structural
488 variants may provide an additional mechanism to increase genetic variation during
489 infection. Here, we found that new insertions of insertion sequences (IS) are strongly
490 enriched during invasive infection. However, despite this 20-fold enrichment, IS
491 insertions remained a rare source of variation even within invasive strains and
492 appeared to have a selective contribution to adaptation (i.e. limited to specific loci

493 such as *agrC*). Similarly, large deletions and copy number variants appeared to play
494 a less prominent role in adaptation, although we didn't include them in our
495 enrichment analysis,
496
497 Together with the enrichment for loss-of function mutations, which is another feature
498 of evolution within the invasive population in our analysis, these IS movements
499 suggest that a pattern of reductive evolution emerges during within-host evolution of
500 invasive *S. aureus*. This excess of genome degradation might be related to less
501 effective purifying selection in the invasive population due to a decrease in effective
502 population size and a shorter evolutionary timescale (84). However, our data indicate
503 that these changes converge to specific genes, operons and pathways, suggesting
504 an adaptative benefit. Reductive evolution has been described in several
505 "commensal-to-pathogen" settings (49). Although niche adaptation through reductive
506 evolution has been described in extracellular pathogens (91), a smaller (reduced)
507 genome is an hallmark of obligate intracellular endosymbiotic bacteria (92). Since it
508 appears that invasive *S. aureus* is able to reside intracellularly (promoting
509 dissemination through mobile phagocytes during *S. aureus* sepsis (93, 94), and
510 immune evasion), it is plausible that this pattern of reductive evolution reflects an
511 adaptation of invasive *S. aureus* to an invasive and intracellular lifestyle, as it has
512 been shown for other facultative intracellular pathogens such as non typhoidal
513 *Salmonella* (19). However, it is possible that these signatures of reductive evolution
514 might be only temporary, as genome degradation might be present only in a minority
515 of strains or be reversible; moreover, loss-of-function mutations are expected to be
516 more likely than gain-of-function mutations.
517

Beside reductive evolution, another distinctive feature of within-host evolution during invasive infection were intergenic mutations (both point mutations and IS insertions). In a within-host evolution study of *S. pneumoniae* colonisation, it was shown that intergenic sites were under convergent evolution (10). Mutations in promoter sequences of some core genes can play an important role in antibiotic resistance as it was repeatedly shown for *pbp4* and resistance to beta-lactam antibiotics (95). The role of intergenic mutations in within-host evolution was shown in a study of *P. aeruginosa* infection, where convergent evolution targeted several intergenic regulatory regions including upstream of antibiotic resistance genes (24).

Previous work on within-host evolution by our group (included in this analysis) has established that *agrA* mutations are significantly enriched upon transition from colonisation to infection (12). In addition, we have shown through genomics and targeted mutagenesis that mutations in key genes such as *walKR* (41) and *rpoB* (96) play a key pathoadaptive role in selected cases of persistent *S. aureus* infections. In this study, we increased our ability to discover potential targets of adaptation by analysing several mechanisms of genetic variation and applying several layers of annotation. As compared to previous work on *S. aureus*, this approach provides a higher-resolution picture of within-host evolution and adaptation. Importantly, this analysis remains robust after removing more than 1,000 sequences from the largest within-host study included (Figure 3 – figure supplement 6). We increase here the generalisibility of our findings. We expand the list of genes targeted by convergent evolution and show that there are distinctive adaptation pathways in colonising and invasive populations. We confirm that the dominantly mutated loci belonged to the *agr* locus, in particular *agrA* and *agrC*. This finding is consistent with a large body of

543 literature that predated the genomic era (97), that supports the role of the *agr* locus
544 as the master regulator of gene expression in *S. aureus*. *Agr*-mediated adaptation
545 was so important that we found a highly significant enrichment of *agr* mutations arros
546 all type variants, including within colonising strains (type C>C variants). Shopsin *et*
547 *a.l* showed that ~10% of healthy *S. aureus* carriers held an agr-defective strain and
548 that prior hospitalisation was significantly associated with agr-defective status,
549 suggesting prior adaptive pressures (98).
550
551 Consistent with the distinctive general patterns of evolution displayed during invasive
552 infection, some genes and loci were specifically mutated within invasive strains.
553 Some of these genes were emerging targets of *S. aureus* pathogenesis *in vivo*, such
554 as *purR* and *yjbH*, that were not singled out in previous within-host evolution
555 investigations. Others were known determinants of antibiotic resistance, including
556 *mprF*, *rpoB* and the *walKR* operon. This underscores the crucial role of antibiotic
557 exposure in shaping adaptive evolution during invasive infection. A recent study of
558 within-host evolution during cystic fibrosis found that resistance genes were hotspots
559 of convergent evolution in this population, which is frequently treated with antibiotics
560 and shows features of phenotypic adaptation (25).
561
562 While most mutations in adaptive loci were substitutions within the coding sequence,
563 about 40% of *walKR* operon mutations were located outside of the coding regions of
564 *walR* and *walk*, emphasising the need to study intergenic mutations and mutations
565 throughout an operon to capture adaptive signatures. This observation highlights the
566 importance of expanding the analysis of intergenic mutations for the detection of
567 adaptive mutations, in particular those linked to antibiotic resistance.

If within-host evolution represents adaptative evolution it is possible that adaptation involved an accumulation of mutations and possibly epistatic mechanisms. Our data show that some mutations are specific for invasive strains; these mutations may reflect late adaptation, occurring after evolution during colonisation in the nose and upon transition from colonisation to infection, and thus occurring after adaptive mutations were acquired during earlier stages. This evolutionary pattern of stepwise adaptation (or adaptive continuum) encompassing the entire within-host evolutionary arch has been well described for cancer (99) and has been also investigated in a study of transition from colonisation to infection (27). One way to capture this is mutation co-occurrence analysis. Here, we show mutation co-occurrence within the *agr* operon, but also co-occurrence of the same mutations in two uncharacterised proteins in *S. aureus*. Our network of mutation co-occurrence linked to *agrAC* mutations might suggest a potential pathway of stepwise adaptation following initial mutations acquisition in the *agr* locus, an hypothesis that has been explored in one of studies included in our analysis (47).

While combining multiple studies allowed us to increase statistical power in order to detect genome-wide convergent signals of adaptation, this approach has some limitations. The quality of the publicly available sequences and metadata can be heterogenous, despite performing quality control assessment, for example due to different read coverage across studies. In addition, detection of structural variants from short reads is not as accurate as from long reads; for example, chromosomal inversions can be missed if they inversion site span is larger than the insert site of the paired-end reads (89).

Ultimately the goal of detecting adaptive signals is to identify new mechanisms of pathogenesis or resistance to therapeutic targets and to inform prediction of clinical outcomes. So far, studies have failed to show consistent associations between specific clinical outcomes and genetic features of infecting (or colonising) *S. aureus* strains. This might be related to the dominance of host / environmental factors, but it could also be linked to the limited power of studies performed so far. By contrast, within-host evolution studies are an elegant approach to identify signatures of adaptation that might be candidate markers of important clinical outcomes, such as infection risk in case of colonisation or treatment failure in case of infection. Here, we show that adaptation signatures are at least partially specific to colonisation, infection and upon transition from colonisation to infection, and that adaptive changes are more frequent in distinctive infection episodes (complicated bacteraemia, endocarditis). These findings suggest that adaptive signatures might be indicative of important clinical outcomes. In the future, precision medicine in infectious diseases could follow the lead of cancer genomics, where within-host evolution studies have tracked the evolution of cancer clones and enabled the detection of high risk mutations early.

MATERIAL AND METHODS

Literature search

We conducted a search of articles indexed in PubMed before the 11th August 2020 using the keyword “aureus” in combination with either “genomics” or “whole genome sequencing” and with either “within-host evolution” or “in vivo evolution” or “adaptation” or “bacteraemia”. The records retrieved through this search were

618 combined with additional citations identified through other sources. After removing
619 duplicates, this resulted in 815 citations that were screened based on following
620 inclusion criteria: i) Whole-genome sequencing of human *S. aureus* isolates; ii) > 1
621 *S. aureus* isolates sequenced per individual; iii) Sequences (reads or assemblies)
622 publicly available; iv) Minimum sequences metadata available (either with the
623 manuscript or linked to the sequences): patient ID, date of collection (or collection
624 interval in reference to a baseline isolate), source of the sample. After excluding
625 studies not satisfying the inclusion criteria (730 based on the title, 46 based on the
626 abstract and 15 after reviewing the full text), we kept 24 within-host evolution studies.
627
628 **Extraction of sequences metadata**
629 For each of the included studies, following variables were extracted either from reads
630 metadata (when available) or from the publication/supplementary data: identifier
631 linking the sequences to a patient or an episode of infection, date of collection (when
632 available) or collection interval in reference to a baseline isolate), site of collection of
633 the isolate. Isolates were broadly categorised in “colonising” and “invasive” based on
634 the site of collection, when the information was unambiguous (e.g. “nose” for
635 “colonising” or “blood” for “invasive”). When the information on the body site was not
636 sufficient (e.g “skin” or “lung”), the categorisation was based on further details
637 provided in the publication. When available, phenotypic metadata and antibiotic
638 treatments were also extracted from the publication. We used clinical and site data to
639 classify colonisation episodes in “nasal carriage”, “atopic dermatitis” and “cystic
640 fibrosis” and infection episodes in “skin infection” (skin infection site surgical site
641 infection without other foci), “osteoarticular infection” (bone/join infection without
642 other foci), “bacteraemia without focus” (bloodstream infection, no other foci, expect

643 for vascular catheter or skin), “bacteraemia with focus (bloodstream infection with
644 other focus involving the lung, nervous system, bone and joints or internal organs),
645 and “endocarditis” (based on diagnosis reported in the publication or in the clinical
646 metadata).
647
648 **Sequences processing**
649 Sequences (reads and assemblies) and metadata were downloaded from the
650 European Nucleotide Archive (ENA) and the National Center for Biotechnology
651 Information (NCBI), respectively using the BioProject accession or the genome
652 accession. Quality assessment of the reads was performed by calculating mean read
653 depth and the fraction of *S. aureus* reads using Kraken 2, v2.0.9-beta (100) and by
654 extracting metrics from reads assemblies constructed using Shovill, v1.1.0
655 (https://github.com/tseemann/shovill) and annotated using Prokka, v1.14.6 (101).
656 Sequence type (ST) was inferred from the assembly using Mlst, v2.19.0
657 (https://github.com/tseemann/mlst) and resistance genes were detected using
658 Abricate, v1.0.1 (https://github.com/tseemann/abricate). Reads were discarded if the
659 mean coverage depth was below 35, the majority of reads were not *S. aureus* or the
660 size of the assembly was below 2.6 megabases. Assemblies downloaded from the
661 NCBI repository were discarded if the genome size was below 2.6 megabases.
662
663 **Sequences from the CAMERA2 trial**
664 We collected *S. aureus* strains from bacteraemia episodes included in the
665 CAMERA2 trial (Combination Antibiotics for Methicillin Resistant *Staphylococcus*
666 *aureus*), where at least 2 strains per episode were available. The CAMERA2 trial
667 was performed between 2015 and 2018 in Australia, New Zealand, Singapore and

Israel, and randomised participants with methicillin-resistant *S. aureus* (MRSA) bacteraemia to either monotherapy with vancomycin or daptomycin or combination therapy with vancomycin or daptomycin plus an antistaphylococcal beta-lactam (flucloxacillin, cloxacillin or cefazolin) (26). Strains were isolated from -80C glycerol onto horse-blood agar. Species was confirmed using Matrix-assisted laser desorption/ionization time-of-flight (MALDI-TOF) mass spectrometry (MS). Bacterial whole-genome sequencing was performed from from single colonies on the Illumnina NextSeq platform. Reads were checked for quality, assembled and annotated as described above.

Global phylogeny

To generate a global alignment of all sequences, reads and shredded assemblies were mapped to reference genome USA300 FPR3757 (assembly accession: GCF_000013465.1) (using Snippy, v4.6.0 (https://github.com/tseemann/snippy). The core genome alignment was obtained using Snippy; sites with > 10% gaps were removed using Goalign (102) and constant sites were removed using SNP-sites (103), for a final length of 186,825 bp. A maximum-likelihood phylogenetic tree of 2,590 sequences (those kept in the analysis after excluding genetically unrelated strains, see below) was inferred using IQ-TREE, v2.0.3 (104).

Variant calling

We have previously shown that the accuracy of variant calling in within-host evolution analyses is improved when mapping reads to an internal draft assembly as opposed to a closely related closed genome (17). Here, we applied the same approach, where we selected the internal reference among the sequences from the

same patient or episode. When available, the oldest colonising strain was selected. When only sequences from invasive strains were available, the oldest strain (baseline strain) was selected. When multiple sequences were available per sample (e.g multiple colonies sequenced per plate) or at the same date, the reference was randomly selected among them. Snippy with default parameters (minimum reads coverage 10, minimumread mapping quality 60, minimum base quality 13) was used for variant calling. To further improve the accuracy of the calls, we masked variants called from reference reads and those at positions where reference reads had a coverage below 10 (using the BEDTools suite (105)).

Filtering of genetically unrelated sequences

The threshold for removing genetically unrelated sequences was set empirically at 100 episode-specific variants based on the upper Tukey's fence of the distribution of the number of variants in same-episode isolates belonging to the same ST (Figure 2 – figure supplement 1).

Detection of chromosome structural variants

Using BWA-MEM, reads and shredded contigs were aligned to the closest available complete genome (either internal to the dataset or selected from the NCBI repository based on the mash distance). To detect large deletions (>= 500 bp), reads coverage was compared between the internal reference and the sequences within every episode using BEDTools, as described in (17). To detect new insertion sequences (IS) insertins, split reads were extracted, filtered and annotated as described in (17). We used the R package CNOGpro (106) to detect 1000 bp windows with an estimated copy number above one as compared to the internal reference. The

718 package calculates the reads coverage per sliding windows of the chromosome,
719 performs a GC bias normalisation and infers copy number state using a Hidden
720 Markow Model. We ran the package with default parameters, with the exception of
721 the length of the sliding window that was set at 1000 bp. As with deletions, we used
722 BEDTools to subtract regions of the internal reference that had already an increased
723 copy number.
724
725 **Internal variant annotation**
726 To ensure a consistent annotation of mutated genes across independent episodes,
727 we clustered amino-acid sequences using CD-HIT, v4.8.1 with an identity threshold
728 of 0.9. The BEDTools suite was used to annotate mutated intergenic regions with
729 upstream and downstream coding regions and the distance separating the mutation
730 from the start or the end of the gene. For the operon analysis, intergenic mutations
731 were classified according to their location within a presumed promoter based on
732 blasting the sequence of unique promoters (as determined in (57)) on the draft
733 assembly of the internal reference. Phage genes were annotated using blastp and
734 the PhageWeb database (http://computationalbiology.ufpa.br/phageweb/).
735
736 **Variant annotation using reference strain FPR3757**
737 To compare mutated genes across separated episodes we used blastp to identify
738 homologs of each CD-HIT cluster of mutated genes in USA300 FPR3757. Genes in
739 FPR3757 were further annotated using the database provided in the AureoWiki
740 repository (107), operon annotations of FPR3757 were retrieved from Microbes
741 Online (108). Only protein-altering variants in genes with FPR3757 homologues

742 (excluding plasmid genes and phage genes) were kept for the analysis of
743 convergence at gene and operon level and the gene enrichment analysis.
744
745 **Classification of variants.**
746 Mutational and structural variants were classified in to type C>C (within colonising
747 strains), type C>I (between colonising and invasive strains) and type I>I (within
748 invasive strains) as follows: all variants arising in colonising strains were classified as
749 type C>C, while variants among invasive strains were classified as type C>I if they
750 were found in a baseline invasive strain (defined as the oldest invasive strain; when
751 multiple sequences were available at same time, the baseline invasive strain was
752 selected randomly), and as type I>I if they were found between invasive strains but
753 not on the baseline invasive strain. This approach is based on the assumption that
754 co-infection or superinfection is rare, as we have shown previously for bacteraemia
755 (17).
756
757 **Calculation of the neutrality index.**
758 A modified McDonald-Kreitman table was compiled a described in (109), where a
759 ratio was calculated between non-synonymous, protein-truncating, IS insertions,
760 intergenic and deletion variants and synonymous variants. The neutrality index was
761 obtained by dividing the ratio calculated above for type C>I (colonsing-invasive) and
762 type I>I (invasive-invasive) by the ratio for type C>C (colonising-colonising) variants,
763 that were used as reference group. Significance was tested by Fisher test.
764
765 **dN/dS analysis**

We used the R package dNdScv (110) to obtain dN/dS ratios for non-synonymous mutations, indels and missense mutations (stop codons) for all FPR3757 genes, based on variants called when mapping all reads on FPR3757 and after subtracting variants from the internal reference reads and variants in positive where internal reference reads had a low coverage. Since this analysis could be hampered by potential false-positive variants resulting from mapping reads on a single reference (17), we also used our curated list of within-host mutations obtaind from episode-specific variant calling to calculate crude dN/dS ratios by dividing the number of protein modifying mutations by the number non-synonymous mutations and computed p values by Fisher exact test as in (25).

Gene and operon enrichment analysis.

We calculated the enrichment of protein-altering mutations across all coding regions of FPR3757 (excluding plasmid genes and phage genes) using the approach described in (12). The variant enrichment per gene *i* was calculated as follows: $(N_i/L_i)/(\Sigma_n/\Sigma_l)$, where N_i is the number of variants per gene *i*, L_i is the length of gene *i*, Σ_n is the total number of variants and Σ_l the total length of the genes. We used Poisson regression to model the number of variants per gene *j* under the null hypothesis (no enrichment), as as defined by the equation $\lambda_0 L_{j,}$ where λ_0 is the expected number of variants in any gene and L_j is the the gene length. Under the alternative hypothesis (enrichment of variant in gene *i*), the estimated number of variants is $\lambda_i L_i$ for gene *i,* and $\lambda_1 L_j$ for any other gene *j*. The model parameters $\lambda_{0,}$ $\lambda_{1,}$ λ_l were estimated using maximum likelihood and tested for significance using the likelihood ratio test. The genome-wide significance cut-off was calculated using the Bonferroni correction (0.05 divided by the number of unique genes or operons) and

the suggestive significance cut-off (1 divided by the number of unique genes or operons), as implemented for bacterial genome-wide associated studies (GWAS) in (22).

Gene set enrichment analysis

For used the PANNZER plateform (111), to retrieve a gene ontology annotation of FPR3757 based on the GO terms. We modified the “antibiotic response” category by adding a curated list of antibiotic resistance genes downloaded from the NCBI AMR gene reference database (70). The gene set enrichment analysis (GSEA) was performed as implemented in the R package clusterProfile (112). Genes with a FPR3757 homolog were ranked according to the significance of the enrichment of protein-modifying mutations (gene enrichment analysis, see above) and the GSEA was carried out with a minimum gene set size of 10 and using the false discovery rate (FDR) method for adjustement for multiple testing.

Mutation co-occurence analysis

To detect co-occurrence of mutations and mutated genes across independent episodes, we constructed a co-occurrence matrix using the R package cooccur (113). A co-occurrence of mutations or mutated genes in at least two independent episodes was interpreted as convergent and as a sign of potential epistatic interaction. The network of co-occurrence of mutated genes was visualised using the R package ggraph (https://cran.r-project.org/web/packages/ggraph/index.html)

Network analysis of adaptation signatures

The pairwise calculation of the Jaccard index between set of mutated genes was performed in R. The calculations were performed both with the entire set of mutated FPR3757 genes and with the 20 most significantly enriched genes in each group of variants. A network of shared mutated genes between independent episodes was constructed using ggraph, where edges represented episode connections based on rthe Jaccard index. We used the R package tidygraph to extract the node centrality (function centrality_degree()) as a summary measure of the degree of adaptation of the episodes. The network graph and analysis was performed for each group of variants separately.

Data availability

The CAMERA2 isolates reads included in this study are available in the European Nucleotide Archive under Bioproject accession no. PRJEB50796.

Code availability

Scripts used to call mutations and structural variants, annotate all variants and perform the gene enrichment analysis are deposited on github at https://github.com/stefanogg/staph_adaptation_paper

FIGURES

Figure 1. Overview of the *S. aureus* within-host evolution analysis framework. (A) Simulated phylogenetic tree illustrating within-host evolution of *S. aureus* colonisation and infection. This model assumes two genetic bottlenecks (dotted lines); upon transmission, and upon transition from colonisation to invasive infection.

(B) Sites and timing of within-host samples and number of genomes per sample define five prototypes of within-host evolution studies, each with colonising-colonising, colonising-invasive or invasive-invasive comparisons in different combinations: from top to the bottom: multiple colonising samples and one invasive samples; one colonising and one invasive sample; multiple colonising samples; multiple invasive samples; multiple colonising and invasive samples. (C) Approach to capture signals of adaptation across multiple independent episodes of colonisation/infection through detection of multiple genetic mechanisms of adaptation from short reads data and multi-layered functional annotation of the genetic variants using multiple databases including characterisation of intergenic regions (promoters), operon prediction, and gene ontology (GO). (D) Statistical framework for the gene, operon and gene set enrichment anlaysis. Counts of independent mutations with likley impact on the protein sequence (non-synonymous substitutions, frameshifts, stop codon mutations, IS insertions) were computed for each genes with a FPR3757 homolog. Gene counts (with the addition of intergenic mutations in promoter regions) were aggregated in operons and gene ontologies. Gene and operon counts were used to fit Poisson regression models to infer mutation enrichment and significance of the enrichment. Gene ontologies counts and gene enrichment significance were used to run a gene-set-enrichment analysis (GSEA). To illustrate the approach, the example of the gene *walR* is provided in italic.

Figure 2. (A) Maximum-likelihood phylogenetic tree of 2,590 *S. aureus* sequences included in the study. The tree is annotated (starting from the inner circle) with the most prevalent sequence types (ST), presence/absence of the *mecA* gene, compartment of isolation (colonising or invasive) and year of publication. (B) Summary of 396 independent episodes of *S. aureus* colonisation or infection

863 categorised according to whether they allowed comparing colonising-colonising
864 (C>C), colonising-invasive (C>I) or invasive-invasive (I>I) strains, or a combination of
865 them. (C) Evidence of a distinctive pattern of adaptation in late infection-adapted
866 strains (type I>I variants). For each type of comparison (type C>C, colonising-
867 colonising; type C>I, colonising-invasive; type I>I, invasive-invasive), the cumulative
868 curves display the accrued number of intergenic mutations, truncating mutations, IS
869 insertions and large deletions as a function of the total number of mutations. Genetic
870 events were counted once per episode, regardless of the number of strains with the
871 mutation. The sequence of mutations events in the cumulative curves is random.
872 **Figure 2 - figure supplement 1.** Number of episode-specific variants in same-
873 episode strains having the same sequence type (ST) as the internal reference vs.
874 isolates with a different ST. The dashed line represents the mutation threshold used
875 to remove genetically unrelated strains with the same episode.
876 **Figure 2 - figure supplement 2.** Distribution of new IS insertions by classification of
877 the transposase and by major sequence types (ST). (A) Distribution of the 9 major
878 ST among 2,590 strains. (B) Number of independent IS insertions by ST group and
879 type of transposase.
880 **Figure 3.** Top 20 genes with the most significant mutation enrichment across the
881 entire dataset. (A) Significance of the enrichment for protein-altering mutations. The
882 dashed line depicts the Bonferroni-corrected significance threshold, red circles and
883 blue circles represent genes with p values below and above the Bonferroni
884 threshold, respectively. (B) Enrichment of protein-altering mutations (C) Bar plots of
885 independent mutations separated in 3 panels according to the type of variant (type
886 C>C: colonising-colonising; type C>I: colonising-invasive; type I>I: invasive-invasive)

887 and coloured according to the class of mutation. (D) Gene maps with type and
888 positions of mutations.
889 **Figure 3 - figure supplement 1.** Mapping of mutations in the 10 most significantly
890 enriched mutated genes across the entire dataset. The maximum-likelihood
891 phylogenetic tree was inferred from the core genome alignment of 2,590 isolates.
892 **Figure 3 - figure supplement 2. dN/dS values for non-synonymous mutations**
893 **(A), indels (B) and nonsense mutations (stop codons) (B) for FPR3757 genes.**
894 Only the 20 most significant genes with positive selection (dN/dS for missense
895 mutations > 1) are shown.
896 **Figure 3 - figure supplement 3.** Most frequently deleted genes in large deletions.
897 **Figure 3 - figure supplement 4.** Most frequently enriched genes in copy number
898 variations.
899 **Figure 3 - figure supplement 5.** Gene convergence analysis of all mutated genes
900 (i.e. including both genes with FPR3757 homolog and no FPR3757 homolog). Top
901 20 genes with the most significant mutation enrichment across the entire dataset. (A)
902 Significance of the enrichment for protein-altering mutations. The dashed line depicts
903 the Bonferroni-corrected significance threshold, red circles and blue circles represent
904 genes with and without FPR3757 homolog, respectively. (B) Enrichment of protein-
905 altering mutations (C) Bar plots of independent mutations separated in 3 panels
906 according to the type of variant (type C>C: colonising-colonising; type C>I:
907 colonising-invasive; type I>I: invasive-invasive) and coloured according to the class
908 of mutation. (D) Gene maps with type and positions of mutations.
909 **Figure 3 - figure supplement 6.** Gene convergence analysis after removing
910 variants in strains included in Young et al, eLIFE 2017, the largest collection of this
911 analysis (1,078 strains, 105 episodes). Top 20 genes with the most significant

912 mutation enrichment across the entire dataset. (A) Significance of the enrichment for
913 protein-altering mutations. The dashed line depicts the Bonferroni-corrected
914 significance threshold, red circles and blue circles represent genes with p values
915 below and above the Bonferroni threshold, respectively. (B) Enrichment of protein-
916 altering mutations (C) Bar plots of independent mutations separated in 3 panels
917 according to the type of variant (type C>C: colonising-colonising; type C>I:
918 colonising-invasive; type I>I: invasive-invasive) and coloured according to the class
919 of mutation. (D) Gene maps with type and positions of mutations.

920 **Figure 4. Top 20 operons with the most significant mutation enrichment across**
921 **all dataset.** (A) Significance of the enrichment for protein-altering mutations. The
922 dashed line depicts the Bonferroni-corrected significance threshold, red circles and
923 blue circles represent operons with p values below and above the Bonferroni
924 threshold, respectively. (B) Enrichment of protein-altering mutations (C) bar plots of
925 independent mutations separated in 3 panels according to the type of variant (type
926 C>C: colonising-colonising; type C>I: colonising-invasive; type I>I: invasive-invasive)
927 and coloured according to the class of mutation. Mutations were considered
928 independent if they occurred in separate episodes of either colonisation or invasive
929 infection. (D) operon maps with positions of the mutations (relative to the start of the
930 first gene of the operon). Operons are labelled with the names of the genes included,
931 longer labels were shorted for clarity (see Supplementary file 5 for details).

932 **Figure 5.** Modified volcano plot displaying enrichment (x axis) and significance of
933 enrichment (y axis) within type C>C, type C>I and type I>I variants. The horizontal
934 dashed line depicts the Bonferroni-corrected significance threshold and dotted line
935 shows the suggestive significance threshold. Labels indicate genes with significance

of enrichment below the suggestive threshold . Genes are coloured in red if the p value is below the Bonferroni-corrected threshold and in blue otherwise.

Figure 5 - figure supplement 1. Modified volcano plot displaying enrichment (x axis) and significance of enrichment (y axis) for FPR3757 operons across the entire dataset, type CC, type CI and type II variants. The horizontal line depicts the Bonferroni-corrected significance threshold. Genes are coloured in red if the p value is below the Bonferroni-corrected threshold and in blue otherwise. Operons are labelled if they were significantly enriched or reached near significance.

Figure 5 - figure supplement 2. Gene-set enrichment analysis (GSEA) for protein-modifying mutations in type CC, type CI and type II variants. (A) Gene ontologies (minimum set size 10 for a total of 110 categories) ordered by normalised enrichment score (NES). Ontologies with negative enrichment were excluded. Dark blue bars indicate a significant p value after false discovery rate (FDR) correction (B) Dot plot of 9 significantly enriched ontologies among type II variants.

Figure 6. Network of mutations co-occurence. The width and colour of the edges represent the strength of the co-occurrence of mutated genes on the same strain (thin and blue, 2 independent co-occurences; thick and orange, 3 independent co-occurences).

Figure 7. Clinical correlates of adaptive signatures within colonising (type C>C, panels A-C) and invasive (type I>I, panels D-F) bacterial populations. Adaptation was inferred by computing the Jaccard index of shared mutated genes between independent episodes, followed by network analysis of infection episodes pairs. The node centrality measure was used as an indicator of adaptation. To avoid overinflation of mutated genes the calculation was limited to the 20 most significantly enriched genes within each group of mutations. (A, D) Density of centrality values

961 across colonisation (panel A) and infection categories (panel D). (B, E) Number and
962 proportion of adaptive episodes. An adaptive episode was defined by a centrality >
963 0. (C, F) Distribution of mutations in the 20 most significantly enriched genes across
964 categories of colonisation (panel C) and infection (panel F).
965 **Figure 7 - figure supplement 1.** Clinical manifestations and infection sites of
966 invasive episodes, grouped by the infection syndromes classification used for the
967 adaptation analysis.
968 **Figure 7 - figure supplement 2.** Network of colonisation/infection episodes for type
969 CC (panel A), type CI (panel B) and type II variants (panel C). Nodes indicate
970 independent episodes, colored based on the clinical syndrome, edges show
971 connections based on shared mutated genes (the width of the connection is
972 proportional to the Jaccard index).
973
974

975 **TABLES**

976 **Table 1.** Microbiological and clinical characteristics of the colonisation and infection

977 episodes included in the within-host evolution analysis

	Strains (n= 2590)	Episodes (n = 396)
Sequence type		
30	342 (13.2%)	43 (10.9%)
22	277 (10.7%)	44 (11.1%)
5	271 (10.5%)	42 (10.6%)
45	198 (7.6%)	38 (9.6%)
15	156 (6.0%)	4 (3.5%)
1	133 (5.1%)	14 (3.5%)
93	110 (4.2%)	29 (7.3%)
8	107 (4.1%)	18 (4.5%)
239	100 (3.9%)	29 (7.3%)
Other	896 (34.6%)	125 (31.6%)
***MecA* positive**	1001 (38.6%)	207 (52.3%)
Infection syndrome		
Skin infection	204 (7.9%)	32 (8.1%)
Osteoarticular infection	77 (3.0%)	17 (4.3%)
Bacteraemia without focus	588 (22.7%)	152 (38.4%)
Bacteraemia with focus	331 (12.8%)	85 (21.5%)
Endocarditis	197 (7.6%)	44 (11.1%)
No invasive strains		66 (16.7%)
Colonisation syndrome		
Nasal carriage	974 (37.6%)	166 (42%)
Cystic fibrosis	57 (2.2%)	9 (2%)

Atopic dermatitis	162 (6.3%)	9 (2%)
No colonising strains		212 (54%)

978

979 **Table 1 – table supplement 1.** List of within-host studies included in the analysis.

980

Author, year	PMID	N independent episodes	N sequences	Ref
Gao W, 2015	28348811	1	18	(23)
Howden BP, 2011	22102812	5	10	(41)
Young BC, 2012	22393007	3	167	(27)
Golubchik, 2013	23658690	13	120	(43)
Burd EM, 2014	24850355	1	3	(44)
Rishishwar L, 2016	27446992	1	3	(33)
Trouillet-Assant S, 2016	26918656	3	6	(29)
Young BC, 2017	29256859	105	1078	(12)
Rouard C, 2018	30275089	1	3	(32)
Langhanki L, 2018	30348081	1	2	(38)
Altman DR, 2018	30061376	10	23	(47)
Giulieri SG, 2018	30103826	49	111	(17)
Benoit JB, 2018	29723202	8	42	(45)
Suligoy CM, 2018	29456969	1	3	(31)
Harkins CP, 2018	28951239	27	248	(42)
Tan X, 2019	30753350	4	8	(30)
Loss G, 2019	31696062	1	2	(36)
Kuroda M, 2019	31474962	1	16	(39)
Azarian T, 2019	31244886	3	44	(46)
Wuethrich D, 2019	30726929	1	5	(28)

Ji S, 2020	32176794	3	20	(40)
Miller CR, 2020	31932377	1	2	(35)
Liu J, 2020	31919223	2	12	(37)
Petrovic Fabijan A, 2020	32066959	12	57	(34)
Tong SYC, 2020	32044943	138	585	(26)

Table 2. Modified McDonald-Kreitman table displaying counts of variants (point mutations and structural variants) and the neutrality index for type C>I and type I>I variants (both compared to type C>C variants).

	Number of variants *(Neutrality index)*		
Classification of variant	**Type C>C**	**Type C>I**	**Type I>I**
synonymous	381	130	155
non-synonymous	978	300 ***(0.9)***	503 ***(1.3)****
intergenic	544	197 ***(1.1)***	549 ***(2.5)****
truncating	197	58 ***(0.9)***	190 ***(2.4)****
IS insertion	17	6 ***(1.0)***	137 ***(19.8)****
large deletion	76	17 ***(0.6)****	122 ***(3.9)****

Values are counts of independent mutations. The neutrality index is shown in brackets in italic.
Significance testing: *: $p < 0.05$; ** $p < 0.005$

Table 3. Genome-wide significant gene signatures of within-host evolution. The genes shown reached genome-wide significance in the entire dataset or in either type C>C, type C>I or type I>I variants.

Gene	**p value (whole dataset)**	**Description**	**N independent mutations**			**Significance**
			Type C>C	**Type C>I**	**Type I>I**	

*agrA***	7.04 x 10^{-28}	accessory gene regulator protein A	5**	9**	8**	Part of the agr quorum sensing system, which is the master regulator of virulence factors expression in *S. aureus*. Recurrent mutations associated with invasive disease.
*agrC***	2.84 x 10^{-10}	accessory gene regulator protein C	4	2	6**	Histidine kinase, receptor for extracellular autoactivating peptide (AIP). Phosphorylates agrA.
*stp1***	1.13 x 10^{-7}	protein phosphatase 2C domain-containing protein	3	2	3	Associated with vancomycin resistance
*mprF***	4.55 x 10^{-6}	oxacillin resistance-related FmtC protein	2	0	9**	Main determinant of daptomycin resistance. Association with persistence and immune evasion.
rpoB	7.24 x 10^{-3}	DNA-directed RNA polymerase subunit beta	1	1	7**	Association with rifampicin resistance, but selection in the absence of rifampicin exposure can happen (R503H). Co-resistance to vancomycin, daptomycin, oxacillin. Association with persistence.

992 ** significant enrichment (above the Bonferroni-corrected cut-off, see methods)

Table 3 – table supplement 1. Gene signatures of within-host evolution with suggestive significant enrichment. The genes shown reached the suggestive significance threshold in the entire dataset or in either type C>C, type C>I or type I>I variants.

Gene	p value (whole dataset)	Description	N independent mutations			Significance
			Type C>C	Type C>I	Type I>I	
*sucA**	6.82×10^{-5}	2-oxoglutarate dehydrogenase E1 component	6	2	2	Encodes a subunit of the α-ketoglutarate dehydrogenase of the tricarboxylic acid cycle (TCA cycle)
*saeR**	1.83×10^{-4}	DNA-binding response regulator SaeR	2	1	2	Regulator component of the saeRS two-component system. Virulence regulation.
accB	4.27×10^{-4}	Biotin carboxyl carrier protein of acetyl-CoA carboxylase	3*	1	0	Part of the fatty acid synthesis pathway of *S. aureus*
SAUSA300_1856	6.41×10^{-4}	hypothetical protein	4*	0	0	Putative intracellular protease. No data on *S. aureus*
xpaC	1.38×10^{-3}	hypothetical protein	4*	0	0	Predicted 5-bromo-4-chloroindolyl phosphate hydrolysis protein, no data on *S. aureus*
rpsJ	1.58×10^{-3}	30S ribosomal protein S10	3*	0	0	Mutations at residues 53-60 are associated with tigecycline resistance, at no apparent fitness cost.
SAUSA300_2399	1.68×10^{-3}	ABC transporter ATP-binding protein	4*	0	0	No data on *S. aureus*
walR	2.10×10^{-3}	DNA-binding response regulator	1	0	3*	Part of walKR two-component response regulator. Associated with vancomycin resistance.

yjbH	3.55 x 10^{-3}	Dsba-family protein	1	0	3*	Negative regulator of spx (directs its ClpXP-dependent degradation). Association with antibiotic resistance, virulence regulation and oxidative stress resistance.
purR	3.86 x 10^{-3}	Pur operon repressor	0	1	3*	*purR* mutants: increased biofilm formation and virulence in animal model; higher capacity to invave epithelial cells.
era	5.34 x 10^{-3}	GTP-binding protein Era	0	1	3*	Involved in ribosome assembly and stringent response.
pbp2	7.75 x 10^{-3}	penicillin binding protein 2	6*	0	0	Role in methicillin resistance (PBP2a synergism). Increased expression after oxacillin exposure.
fakA	9.90 x 10^{-3}	hypothetical protein	5*	0	0	Fatty acid kinase. Deletion mutant displayed increased virulence in a murine model of skin infection.
sgtB	2.65 x 10^{-2}	glycosyltransferase	0	0	3*	sgtB mutations in adaptive laboratory evolution experiments upon vancomycin exposure.

997 * suggestive significant enrichment (above the suggestive significance cut-off, see methods)

998

SUPPLEMENTARY FILES

Supplementary file 1. List of colonisation/infection episodes included with publication data (first author, year, PubMed id), number of strains, sites of collection, clinical characterstics, classification of colonisation and infection episodes.

Supplementary file 2. List of strains included with site and date of collection, sequence type, presence of the *mecA* gene, information on whether the strain was designed as internal reference or baseline index strain, mash distance to the internal reference, number of variants called (as compared to the internal reference), sequencing metrics.

Supplementary file 3. List of variants identified annotated with gene, gene sequence, FPR3757 homolog, FPR3757 operon. Point mutations, IS insertions, large deletions and copy number variants are presented separately.

Supplementary file 4. Gene enrichment analysis for all mutated genes with a FPR3757 homolog with number of mutations, gene length, mutation enrichment, p value based on a Poisson regression to model the number of variants per gene. Results are presented separately for the complete dataset and for type C>C, type C>I, and type I>I variants.

Supplementary file 5. Operon enrichment analysis for all FPR3757 operons (i.e. mutated genes that could be assigned to a FPR3757 operon) with number of mutations, operon length, mutation enrichment, p value based on a Poisson regression to model the number of variants per operon. Results are presented separately for the complete dataset and for type C>C, type C>I, and type I>I variants.

Supplementary file 6. Gene set enrichment analysis for mutations in genes aggregated in gene ontologies (GO) categories with enrichment score, normalsied

enrichment score (NES), unadjusted and false-discovery rate (FDR) adjusted p value. Results are presented separately for the complete dataset and for type C>C, type C>I, and type I>I variants.

REFERENCES

1. Tong SY, Davis JS, Eichenberger E, Holland TL, Fowler VG, Jr. Staphylococcus aureus infections: epidemiology, pathophysiology, clinical manifestations, and management. Clin Microbiol Rev. 2015;28(3):603-61.
2. Wertheim HF, Melles DC, Vos MC, van Leeuwen W, van Belkum A, Verbrugh HA, et al. The role of nasal carriage in Staphylococcus aureus infections. Lancet Infect Dis. 2005;5(12):751-62.
3. Krismer B, Weidenmaier C, Zipperer A, Peschel A. The commensal lifestyle of Staphylococcus aureus and its interactions with the nasal microbiota. Nat Rev Microbiol. 2017;15(11):675-87.
4. Proctor RA. Immunity to Staphylococcus aureus: Implications for Vaccine Development. Microbiol Spectr. 2019;7(4).
5. Kuehl R, Morata L, Meylan S, Mensa J, Soriano A. When antibiotics fail: a clinical and microbiological perspective on antibiotic tolerance and persistence of Staphylococcus aureus. J Antimicrob Chemother. 2020;75(5):1071-86.
6. Hood MI, Skaar EP. Nutritional immunity: transition metals at the pathogen-host interface. Nat Rev Microbiol. 2012;10(8):525-37.
7. Marvig RL, Sommer LM, Molin S, Johansen HK. Convergent evolution and adaptation of Pseudomonas aeruginosa within patients with cystic fibrosis. Nature Genetics. 2015;47(1):57-64.
8. Kennemann L, Didelot X, Aebischer T, Kuhn S, Drescher B, Droege M, et al. Helicobacter pylori genome evolution during human infection. Proceedings of the National Academy of Sciences. 2011;108:5033-8.
9. Lieberman TD, Wilson D, Misra R, Xiong LL, Moodley P, Cohen T, et al. Genomic diversity in autopsy samples reveals within-host dissemination of HIV-associated Mycobacterium tuberculosis. Nat Med. 2016;22(12):1470-4.
10. Chaguza C, Senghore M, Bojang E, Gladstone RA, Lo SW, Tientcheu PE, et al. Within-host microevolution of Streptococcus pneumoniae is rapid and adaptive during natural colonisation. Nat Commun. 2020;11(1):3442.
11. Paterson GK, Harrison EM, Murray GGR, Welch JJ, Warland JH, Holden MTG, et al. Capturing the cloud of diversity reveals complexity and heterogeneity of MRSA carriage, infection and transmission. Nature Communications. 2015;6(1):6560.
12. Young BC, Wu C-H, Gordon NC, Cole K, Price JR, Liu E, et al. Severe infections emerge from commensal bacteria by adaptive evolution. eLife. 2017;6:e30637.
13. Van Tyne D, Manson AL, Huycke MM, Karanicolas J, Earl AM, Gilmore MS. Impact of antibiotic treatment and host innate immune pressure on enterococcal adaptation in the human bloodstream. Sci Transl Med. 2019;11(487).

14. Lees JA, Kremer PHC, Manso AS, Croucher NJ, Ferwerda B, Serón MV, et al. Large scale genomic analysis shows no evidence for pathogen adaptation between the blood and cerebrospinal fluid niches during bacterial meningitis. Microb Genom. 2017;3(1):e000103.
15. Giulieri SG, Guerillot R, Kwong JC, Monk IR, Hayes AS, Daniel D, et al. Comprehensive Genomic Investigation of Adaptive Mutations Driving the Low-Level Oxacillin Resistance Phenotype in Staphylococcus aureus. mBio. 2020;11(6).
16. Howden BP, Johnson PD, Ward PB, Stinear TP, Davies JK. Isolates with low-level vancomycin resistance associated with persistent methicillin-resistant Staphylococcus aureus bacteremia. Antimicrob Agents Chemother. 2006;50(9):3039-47.
17. Giulieri SG, Baines SL, Guerillot R, Seemann T, Gonçalves da Silva A, Schultz M, et al. Genomic exploration of sequential clinical isolates reveals a distinctive molecular signature of persistent Staphylococcus aureus bacteraemia. Genome Medicine. 2018;10(1):65.
18. Wheatley R, Diaz Caballero J, Kapel N, de Winter FHR, Jangir P, Quinn A, et al. Rapid evolution and host immunity drive the rise and fall of carbapenem resistance during an acute Pseudomonas aeruginosa infection. Nature Communications. 2021;12(1):2460.
19. Klemm EJ, Gkrania-Klotsas E, Hadfield J, Forbester JL, Harris SR, Hale C, et al. Emergence of host-adapted Salmonella Enteritidis through rapid evolution in an immunocompromised host. Nature Microbiology. 2016;1(3):15023.
20. Vargas R, Freschi L, Marin M, Epperson LE, Smith M, Oussenko I, et al. In-host population dynamics of Mycobacterium tuberculosis complex during active disease. Elife. 2021;10.
21. Gatt YE, Margalit H. Common Adaptive Strategies Underlie Within-Host Evolution of Bacterial Pathogens. Molecular Biology and Evolution. 2020.
22. Lees JA, Croucher NJ, Goldblatt D, Nosten F, Parkhill J, Turner C, et al. Genome-wide identification of lineage and locus specific variation associated with pneumococcal carriage duration. Elife. 2017;6.
23. Gao W, Monk IR, Tobias NJ, Gladman SL, Seemann T, Stinear TP, et al. Large tandem chromosome expansions facilitate niche adaptation during persistent infection with drug-resistant Staphylococcus aureus. Microb Genom. 2015;1(2):e000026.
24. Khademi SMH, Sazinas P, Jelsbak L. Within-Host Adaptation Mediated by Intergenic Evolution in Pseudomonas aeruginosa. Genome Biology and Evolution. 2019;11(5):1385-97.
25. Long DR, Wolter DJ, Lee M, Precit M, McLean K, Holmes E, et al. Polyclonality, Shared Strains, and Convergent Evolution in Chronic CF S. aureus Airway Infection. Am J Respir Crit Care Med. 2020.
26. Tong SYC, Lye DC, Yahav D, Sud A, Robinson JO, Nelson J, et al. Effect of Vancomycin or Daptomycin With vs Without an Antistaphylococcal β-Lactam on Mortality, Bacteremia, Relapse, or Treatment Failure in Patients With MRSA Bacteremia: A Randomized Clinical Trial. JAMA. 2020;323(6):527-37.
27. Young BC, Golubchik T, Batty EM, Fung R, Larner-Svensson H, Votintseva AA, et al. Evolutionary dynamics of Staphylococcus aureus during progression from carriage to disease. Proc Natl Acad Sci U S A. 2012;109(12):4550-5.
28. Wuthrich D, Cuenod A, Hinic V, Morgenstern M, Khanna N, Egli A, et al. Genomic characterization of inpatient evolution of MRSA resistant to daptomycin, vancomycin and ceftaroline. J Antimicrob Chemother. 2019;74(5):1452-4.

29. Trouillet-Assant S, Lelievre L, Martins-Simoes P, Gonzaga L, Tasse J, Valour F, et al. Adaptive processes of Staphylococcus aureus isolates during the progression from acute to chronic bone and joint infections in patients. Cell Microbiol. 2016;18(10):1405-14.
30. Tan X, Coureuil M, Ramond E, Euphrasie D, Dupuis M, Tros F, et al. Chronic Staphylococcus aureus Lung Infection Correlates With Proteogenomic and Metabolic Adaptations Leading to an Increased Intracellular Persistence. Clin Infect Dis. 2019;69(11):1937-45.
31. Suligoy CM, Lattar SM, Noto Llana M, Gonzalez CD, Alvarez LP, Robinson DA, et al. Mutation of Agr Is Associated with the Adaptation of Staphylococcus aureus to the Host during Chronic Osteomyelitis. Front Cell Infect Microbiol. 2018;8:18.
32. Rouard C, Garnier F, Leraut J, Lepainteur M, Rahajamananav L, Languepin J, et al. Emergence and Within-Host Genetic Evolution of Methicillin-Resistant Staphylococcus aureus Resistant to Linezolid in a Cystic Fibrosis Patient. Antimicrob Agents Chemother. 2018;62(12).
33. Rishishwar L, Kraft CS, Jordan IK. Population Genomics of Reduced Vancomycin Susceptibility in Staphylococcus aureus. mSphere. 2016;1(4).
34. Petrovic Fabijan A, Lin RCY, Ho J, Maddocks S, Ben Zakour NL, Iredell JR, et al. Safety of bacteriophage therapy in severe Staphylococcus aureus infection. Nat Microbiol. 2020;5(3):465-72.
35. Miller CR, Dey S, Smolenski PD, Kulkarni PS, Monk JM, Szubin R, et al. Distinct Subpopulations of Intravalvular Methicillin-Resistant Staphylococcus aureus with Variable Susceptibility to Daptomycin in Tricuspid Valve Endocarditis. Antimicrob Agents Chemother. 2020;64(3).
36. Loss G, Simoes PM, Valour F, Cortes MF, Gonzaga L, Bergot M, et al. Staphylococcus aureus Small Colony Variants (SCVs): News From a Chronic Prosthetic Joint Infection. Front Cell Infect Microbiol. 2019;9:363.
37. Liu J, Gefen O, Ronin I, Bar-Meir M, Balaban NQ. Effect of tolerance on the evolution of antibiotic resistance under drug combinations. Science. 2020;367(6474):200-4.
38. Langhanki L, Berger P, Treffon J, Catania F, Kahl BC, Mellmann A. In vivo competition and horizontal gene transfer among distinct Staphylococcus aureus lineages as major drivers for adaptational changes during long-term persistence in humans. BMC Microbiol. 2018;18(1):152.
39. Kuroda M, Sekizuka T, Matsui H, Ohsuga J, Ohshima T, Hanaki H. IS256-Mediated Overexpression of the WalKR Two-Component System Regulon Contributes to Reduced Vancomycin Susceptibility in a Staphylococcus aureus Clinical Isolate. Front Microbiol. 2019;10:1882.
40. Ji S, Jiang S, Wei X, Sun L, Wang H, Zhao F, et al. In-Host Evolution of Daptomycin Resistance and Heteroresistance in Methicillin-Resistant Staphylococcus aureus Strains From Three Endocarditis Patients. J Infect Dis. 2020;221(Suppl 2):S243-S52.
41. Howden BP, McEvoy CR, Allen DL, Chua K, Gao W, Harrison PF, et al. Evolution of multidrug resistance during Staphylococcus aureus infection involves mutation of the essential two component regulator WalKR. PLoS Pathog. 2011;7(11):e1002359.
42. Harkins CP, Pettigrew KA, Oravcova K, Gardner J, Hearn RMR, Rice D, et al. The Microevolution and Epidemiology of Staphylococcus aureus Colonization during Atopic Eczema Disease Flare. J Invest Dermatol. 2018;138(2):336-43.

43. Golubchik T, Batty EM, Miller RR, Farr H, Young BC, Larner-Svensson H, et al. Within-host evolution of Staphylococcus aureus during asymptomatic carriage. PLoS One. 2013;8(5):e61319.
44. Burd EM, Alam MT, Passalacqua KD, Kalokhe AS, Eaton ME, Satola SW, et al. Development of oxacillin resistance in a patient with recurrent Staphylococcus aureus bacteremia. J Clin Microbiol. 2014;52(8):3114-7.
45. Benoit JB, Frank DN, Bessesen MT. Genomic evolution of Staphylococcus aureus isolates colonizing the nares and progressing to bacteremia. PLoS One. 2018;13(5):e0195860.
46. Azarian T, Ridgway JP, Yin Z, David MZ. Long-Term Intrahost Evolution of Methicillin Resistant Staphylococcus aureus Among Cystic Fibrosis Patients With Respiratory Carriage. Front Genet. 2019;10:546.
47. Altman DR, Sullivan MJ, Chacko KI, Balasubramanian D, Pak TR, Sause WE, et al. Genome Plasticity of agr-Defective Staphylococcus aureus during Clinical Infection. Infect Immun. 2018;86(10).
48. Hawkey J, Monk JM, Billman-Jacobe H, Palsson B, Holt KE. Impact of insertion sequences on convergent evolution of Shigella species. PLoS Genet. 2020;16(7):e1008931.
49. Toft C, Andersson SG. Evolutionary microbial genomics: insights into bacterial host adaptation. Nat Rev Genet. 2010;11(7):465-75.
50. McEvoy CR, Tsuji B, Gao W, Seemann T, Porter JL, Doig K, et al. Decreased vancomycin susceptibility in Staphylococcus aureus caused by IS256 tempering of WalKR expression. Antimicrob Agents Chemother. 2013;57(7):3240-9.
51. Schreiber F, Szekat C, Josten M, Sahl HG, Bierbaum G. Antibiotic-induced autoactivation of IS256 in Staphylococcus aureus. Antimicrob Agents Chemother. 2013;57(12):6381-4.
52. Smyth DS, Kafer JM, Wasserman GA, Velickovic L, Mathema B, Holzman RS, et al. Nasal carriage as a source of agr-defective Staphylococcus aureus bacteremia. J Infect Dis. 2012;206(8):1168-77.
53. Wang Y, Bojer MS, George SE, Wang Z, Jensen PR, Wolz C, et al. Inactivation of TCA cycle enhances Staphylococcus aureus persister cell formation in stationary phase. Sci Rep. 2018;8(1):10849.
54. Lopatkin AJ, Bening SC, Manson AL, Stokes JM, Kohanski MA, Badran AH, et al. Clinically relevant mutations in core metabolic genes confer antibiotic resistance. Science. 2021;371(6531):eaba0862.
55. Phaneuf PV, Yurkovich JT, Heckmann D, Wu M, Sandberg TE, King ZA, et al. Causal mutations from adaptive laboratory evolution are outlined by multiple scales of genome annotations and condition-specificity. BMC Genomics. 2020;21(1):514.
56. Mäder U, Nicolas P, Depke M, Pané-Farré J, Debarbouille M, van der Kooi-Pol MM, et al. Staphylococcus aureus Transcriptome Architecture: From Laboratory to Infection-Mimicking Conditions. PLoS genetics. 2016;12(4):e1005962-e.
57. Prados J, Linder P, Redder P. TSS-EMOTE, a refined protocol for a more complete and less biased global mapping of transcription start sites in bacterial pathogens. BMC Genomics. 2016;17(1):849.
58. Both A, Huang J, Qi M, Lausmann C, Weißelberg S, Büttner H, et al. Distinct clonal lineages and within-host diversification shape invasive Staphylococcus epidermidis populations. PLOS Pathogens. 2021;17(2):e1009304.
59. Suligoy CM, Díaz RE, Gehrke AK, Ring N, Yebra G, Alves J, et al. Acapsular Staphylococcus aureus with a non-functional agr regains capsule expression after

passage through the bloodstream in a bacteremia mouse model. Sci Rep. 2020;10(1):14108.
60. Machado H, Seif Y, Sakoulas G, Olson CA, Hefner Y, Anand A, et al. Environmental conditions dictate differential evolution of vancomycin resistance in Staphylococcus aureus. Communications Biology. 2021;4(1):793.
61. Guerillot R, Goncalves da Silva A, Monk I, Giulieri S, Tomita T, Alison E, et al. Convergent Evolution Driven by Rifampin Exacerbates the Global Burden of Drug-Resistant Staphylococcus aureus. mSphere. 2018;3(1).
62. Austin CM, Garabaglu S, Krute CN, Ridder MJ, Seawell NA, Markiewicz MA, et al. Contribution of YjbIH to Virulence Factor Expression and Host Colonization in Staphylococcus aureus. Infection and Immunity. 2019;87(6):e00155-19.
63. Göhring N, Fedtke I, Xia G, Jorge AM, Pinho MG, Bertsche U, et al. New role of the disulfide stress effector YjbH in β-lactam susceptibility of Staphylococcus aureus. Antimicrob Agents Chemother. 2011;55(12):5452-8.
64. Renzoni A, Andrey DO, Jousselin A, Barras C, Monod A, Vaudaux P, et al. Whole genome sequencing and complete genetic analysis reveals novel pathways to glycopeptide resistance in Staphylococcus aureus. PLoS One. 2011;6(6):e21577.
65. Engman J, Rogstam A, Frees D, Ingmer H, von Wachenfeldt C. The YjbH adaptor protein enhances proteolysis of the transcriptional regulator Spx in Staphylococcus aureus. J Bacteriol. 2012;194(5):1186-94.
66. Paudel A, Panthee S, Hamamoto H, Grunert T, Sekimizu K. YjbH regulates virulence genes expression and oxidative stress resistance in Staphylococcus aureus. Virulence. 2021;12(1):470-80.
67. Sause WE, Balasubramanian D, Irnov I, Copin R, Sullivan MJ, Sommerfield A, et al. The purine biosynthesis regulator PurR moonlights as a virulence regulator in Staphylococcus aureus. Proc Natl Acad Sci U S A. 2019;116(27):13563-72.
68. Goncheva MI, Flannagan RS, Sterling BE, Laakso HA, Friedrich NC, Kaiser JC, et al. Stress-induced inactivation of the Staphylococcus aureus purine biosynthesis repressor leads to hypervirulence. Nat Commun. 2019;10(1):775.
69. Goncheva MI, Flannagan RS, Heinrichs DE. De Novo Purine Biosynthesis Is Required for Intracellular Growth of Staphylococcus aureus and for the Hypervirulence Phenotype of a purR Mutant. Infect Immun. 2020;88(5).
70. Feldgarden M, Brover V, Haft DH, Prasad AB, Slotta DJ, Tolstoy I, et al. Validating the AMRFinder Tool and Resistance Gene Database by Using Antimicrobial Resistance Genotype-Phenotype Correlations in a Collection of Isolates. Antimicrob Agents Chemother. 2019;63(11).
71. Levin-Reisman I, Brauner A, Ronin I, Balaban NQ. Epistasis between antibiotic tolerance, persistence, and resistance mutations. Proc Natl Acad Sci U S A. 2019;116(29):14734-9.
72. Skwark MJ, Croucher NJ, Puranen S, Chewapreecha C, Pesonen M, Xu YY, et al. Interacting networks of resistance, virulence and core machinery genes identified by genome-wide epistasis analysis. PLoS Genet. 2017;13(2):e1006508.
73. Wadsworth CB, Arnold BJ, Sater MRA, Grad YH. Azithromycin Resistance through Interspecific Acquisition of an Epistasis-Dependent Efflux Pump Component and Transcriptional Regulator in Neisseria gonorrhoeae. mBio. 2018;9(4).
74. Yokoyama M, Stevens E, Laabei M, Bacon L, Heesom K, Bayliss S, et al. Epistasis analysis uncovers hidden antibiotic resistance-associated fitness costs hampering the evolution of MRSA. Genome Biology. 2018;19(1):94.
75. Phillips PC. Epistasis — the essential role of gene interactions in the structure and evolution of genetic systems. Nature Reviews Genetics. 2008;9(11):855-67.

76. Aseev LV, Boni IV. Extraribosomal functions of bacterial ribosomal proteins. Molecular Biology. 2011;45(5):739.
77. Monk IR, Shaikh N, Begg SL, Gajdiss M, Sharkey LKR, Lee JYH, et al. Zinc-binding to the cytoplasmic PAS domain regulates the essential WalK histidine kinase of Staphylococcus aureus. Nature Communications. 2019;10(1):3067.
78. Cameron DR, Ward DV, Kostoulias X, Howden BP, Moellering RC, Jr., Eliopoulos GM, et al. Serine/threonine phosphatase Stp1 contributes to reduced susceptibility to vancomycin and virulence in Staphylococcus aureus. J Infect Dis. 2012;205(11):1677-87.
79. Trong HNG, Prunier A-L, Leclercq R. Hypermutable and fluoroquinolone-resistant clinical isolates of Staphylococcus aureus. Antimicrobial agents and chemotherapy. 2005;49(5):2098-101.
80. Wheeler NE, Gardner PP, Barquist L. Machine learning identifies signatures of host adaptation in the bacterial pathogen Salmonella enterica. PLoS Genet. 2018;14(5):e1007333.
81. Bailey SF, Blanquart F, Bataillon T, Kassen R. What drives parallel evolution?: How population size and mutational variation contribute to repeated evolution. Bioessays. 2017;39(1):1-9.
82. Bryant JM, Brown KP, Burbaud S, Everall I, Belardinelli JM, Rodriguez-Rincon D, et al. Stepwise pathogenic evolution of Mycobacterium abscessus. Science. 2021;372(6541).
83. Key FM, Khadka VD, Romo-González C, Blake KJ, Deng L, Lynn TC, et al. On-person adaptive evolution of Staphylococcus aureus during atopic dermatitis increases disease severity. bioRxiv. 2021:2021.03.24.436824.
84. Didelot X, Walker AS, Peto TE, Crook DW, Wilson DJ. Within-host evolution of bacterial pathogens. Nat Rev Microbiol. 2016;14(3):150-62.
85. McVicker G, Prajsnar TK, Williams A, Wagner NL, Boots M, Renshaw SA, et al. Clonal expansion during Staphylococcus aureus infection dynamics reveals the effect of antibiotic intervention. PLoS Pathog. 2014;10(2):e1003959.
86. Guerillot R, Li L, Baines S, Howden B, Schultz MB, Seemann T, et al. Comprehensive antibiotic-linked mutation assessment by resistance mutation sequencing (RM-seq). Genome Med. 2018;10(1):63.
87. Peleg AY, Miyakis S, Ward DV, Earl AM, Rubio A, Cameron DR, et al. Whole genome characterization of the mechanisms of daptomycin resistance in clinical and laboratory derived isolates of Staphylococcus aureus. PLoS One. 2012;7(1):e28316.
88. Jiang JH, Dexter C, Cameron DR, Monk IR, Baines SL, Abbott IJ, et al. Evolution of Daptomycin Resistance in Coagulase-Negative Staphylococci Involves Mutations of the Essential Two-Component Regulator WalKR. Antimicrob Agents Chemother. 2019;63(3).
89. Guerillot R, Kostoulias X, Donovan L, Li L, Carter GP, Hachani A, et al. Unstable chromosome rearrangements in Staphylococcus aureus cause phenotype switching associated with persistent infections. Proc Natl Acad Sci U S A. 2019;116(40):20135-40.
90. Laabei M, Uhlemann AC, Lowy FD, Austin ED, Yokoyama M, Ouadi K, et al. Evolutionary Trade-Offs Underlie the Multi-faceted Virulence of Staphylococcus aureus. PLoS Biol. 2015;13(9):e1002229.
91. Stinear TP, Seemann T, Pidot S, Frigui W, Reysset G, Garnier T, et al. Reductive evolution and niche adaptation inferred from the genome of Mycobacterium ulcerans, the causative agent of Buruli ulcer. Genome Res. 2007;17(2):192-200.

92. Batut B, Knibbe C, Marais G, Daubin V. Reductive genome evolution at both ends of the bacterial population size spectrum. Nat Rev Microbiol. 2014;12(12):841-50.
93. Thwaites GE, Gant V. Are bloodstream leukocytes Trojan Horses for the metastasis of Staphylococcus aureus? Nat Rev Microbiol. 2011;9(3):215-22.
94. Surewaard BG, Deniset JF, Zemp FJ, Amrein M, Otto M, Conly J, et al. Identification and treatment of the Staphylococcus aureus reservoir in vivo. J Exp Med. 2016;213(7):1141-51.
95. Basuino L, Jousselin A, Alexander JAN, Strynadka NCJ, Pinho MG, Chambers HF, et al. PBP4 activity and its overexpression are necessary for PBP4-mediated high-level β-lactam resistance. J Antimicrob Chemother. 2018;73(5):1177-80.
96. Gao W, Cameron DR, Davies JK, Kostoulias X, Stepnell J, Tuck KL, et al. The RpoB H(4)(8)(1)Y rifampicin resistance mutation and an active stringent response reduce virulence and increase resistance to innate immune responses in Staphylococcus aureus. J Infect Dis. 2013;207(6):929-39.
97. Novick RP, Geisinger E. Quorum sensing in staphylococci. Annu Rev Genet. 2008;42:541-64.
98. Shopsin B, Drlica-Wagner A, Mathema B, Adhikari RP, Kreiswirth BN, Novick RP. Prevalence of agr dysfunction among colonizing Staphylococcus aureus strains. J Infect Dis. 2008;198(8):1171-4.
99. Abbosh C, Birkbak NJ, Wilson GA, Jamal-Hanjani M, Constantin T, Salari R, et al. Phylogenetic ctDNA analysis depicts early-stage lung cancer evolution. Nature. 2017;545(7655):446-51.
100. Wood DE, Lu J, Langmead B. Improved metagenomic analysis with Kraken 2. Genome Biology. 2019;20(1):257.
101. Seemann T. Prokka: rapid prokaryotic genome annotation. Bioinformatics. 2014;30(14):2068-9.
102. Lemoine F, Gascuel O. Gotree/Goalign : Toolkit and Go API to facilitate the development of phylogenetic workflows. bioRxiv. 2021:2021.06.09.447704.
103. Page AJ, Taylor B, Delaney AJ, Soares J, Seemann T, Keane JA, et al. SNP-sites: rapid efficient extraction of SNPs from multi-FASTA alignments. Microbial Genomics. 2016;2(4).
104. Minh BQ, Schmidt HA, Chernomor O, Schrempf D, Woodhams MD, von Haeseler A, et al. IQ-TREE 2: New Models and Efficient Methods for Phylogenetic Inference in the Genomic Era. Molecular Biology and Evolution. 2020;37(5):1530-4.
105. Quinlan AR, Hall IM. BEDTools: a flexible suite of utilities for comparing genomic features. Bioinformatics. 2010;26(6):841-2.
106. Brynildsrud O, Snipen LG, Bohlin J. CNOGpro: detection and quantification of CNVs in prokaryotic whole-genome sequencing data. Bioinformatics. 2015;31(11):1708-15.
107. Fuchs S, Mehlan H, Bernhardt J, Hennig A, Michalik S, Surmann K, et al. AureoWiki – The repository of the Staphylococcus aureus research and annotation community. International Journal of Medical Microbiology. 2018;308(6):558-68.
108. Dehal PS, Joachimiak MP, Price MN, Bates JT, Baumohl JK, Chivian D, et al. MicrobesOnline: an integrated portal for comparative and functional genomics. Nucleic Acids Res. 2010;38(Database issue):D396-400.
109. Stoletzki N, Eyre-Walker A. Estimation of the Neutrality Index. Molecular Biology and Evolution. 2010;28(1):63-70.

110. Martincorena I, Raine KM, Gerstung M, Dawson KJ, Haase K, Van Loo P, et al. Universal Patterns of Selection in Cancer and Somatic Tissues. Cell. 2017;171(5):1029-41.e21.
111. Törönen P, Medlar A, Holm L. PANNZER2: a rapid functional annotation web server. Nucleic Acids Res. 2018;46(W1):W84-w8.
112. clusterProfiler: an R Package for Comparing Biological Themes Among Gene Clusters. OMICS: A Journal of Integrative Biology. 2012;16(5):284-7.
113. Griffith DM, Veech JA, Marsh CJ. cooccur: Probabilistic Species Co-Occurrence Analysis in R. 2016. 2016;69(Code Snippet 2):17.

ACKNOWLEDGMENTS

The authors declare that they have no competing interests. All data needed to evaluate the conclusions in the paper are present in the paper and/or the Supplementary Materials. This work was supported by a Research Fellowship to BPH and TPS from the National Health and Medical Research Council, Australia. SGG was supported by a PhD scholarship of the University of Melbourne. We acknowledge the CAMERA2 investigators and trial steering committee for sharing sequences and clinical metadata of trial participants with multiple sequential bacteraemia strains.

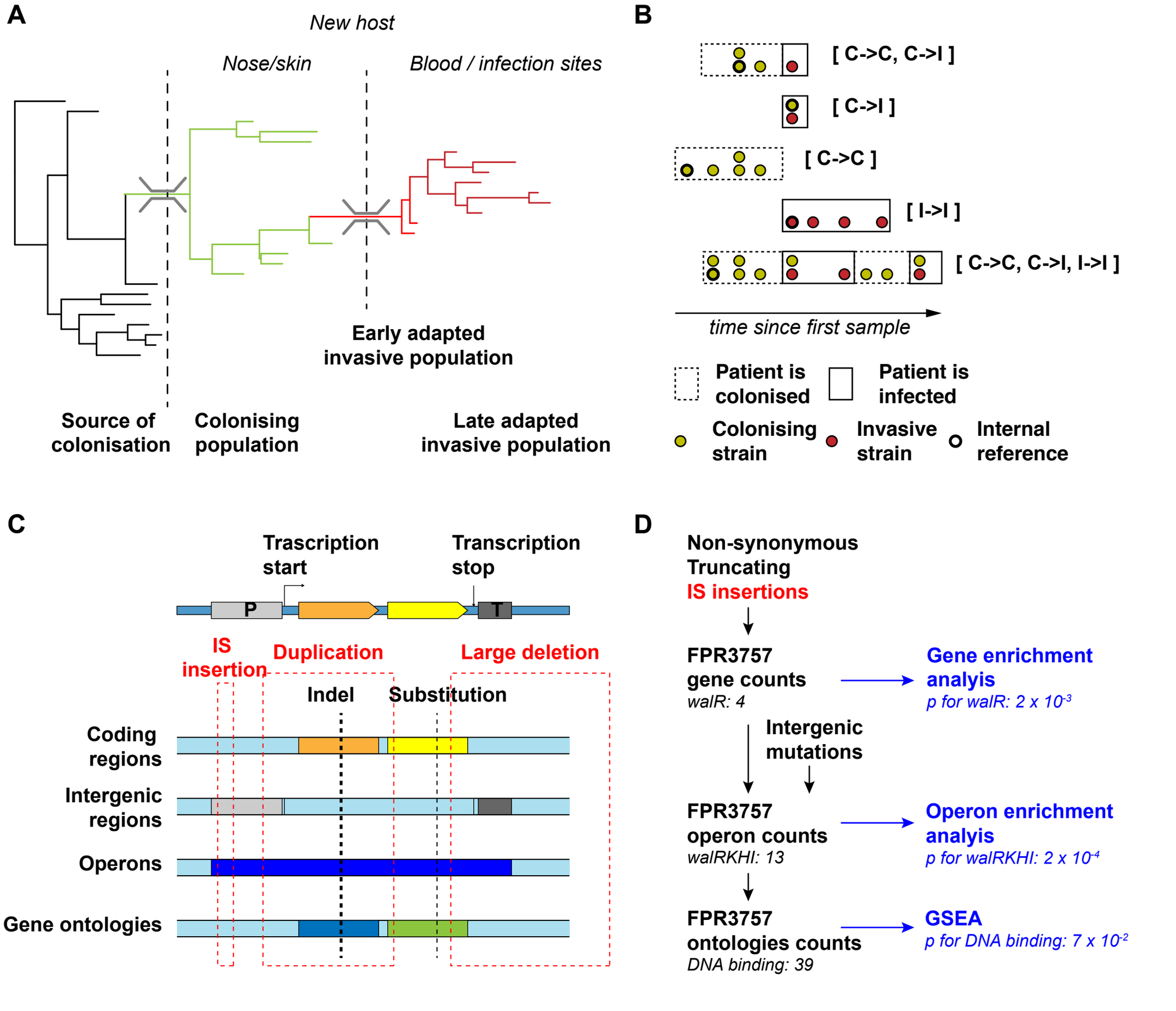
A
New host
Nose/skin
Blood / infection sites
Early adapted invasive population
Source of colonisation
Colonising population
Late adapted invasive population
B
[C->C, C->I]
[C->I]
[C->C]
[I->I]
[C->C, C->I, I->I]
time since first sample
Patient is colonised
Patient is infected
Colonising strain
Invasive strain
Internal reference
C
Trascription start
Transcription stop
P
T
IS insertion
Duplication
Large deletion
Indel
Substitution
Coding regions
Intergenic regions
Operons
Gene ontologies
D
Non-synonymous
Truncating
IS insertions
FPR3757 gene counts
walR: 4
Gene enrichment analyis
p for walR: 2 x 10-3
Intergenic mutations
FPR3757 operon counts
walRKHI: 13
Operon enrichment analyis
p for walRKHI: 2 x 10-4
FPR3757 ontologies counts
DNA binding: 39
GSEA
p for DNA binding: 7 x 10-2

A

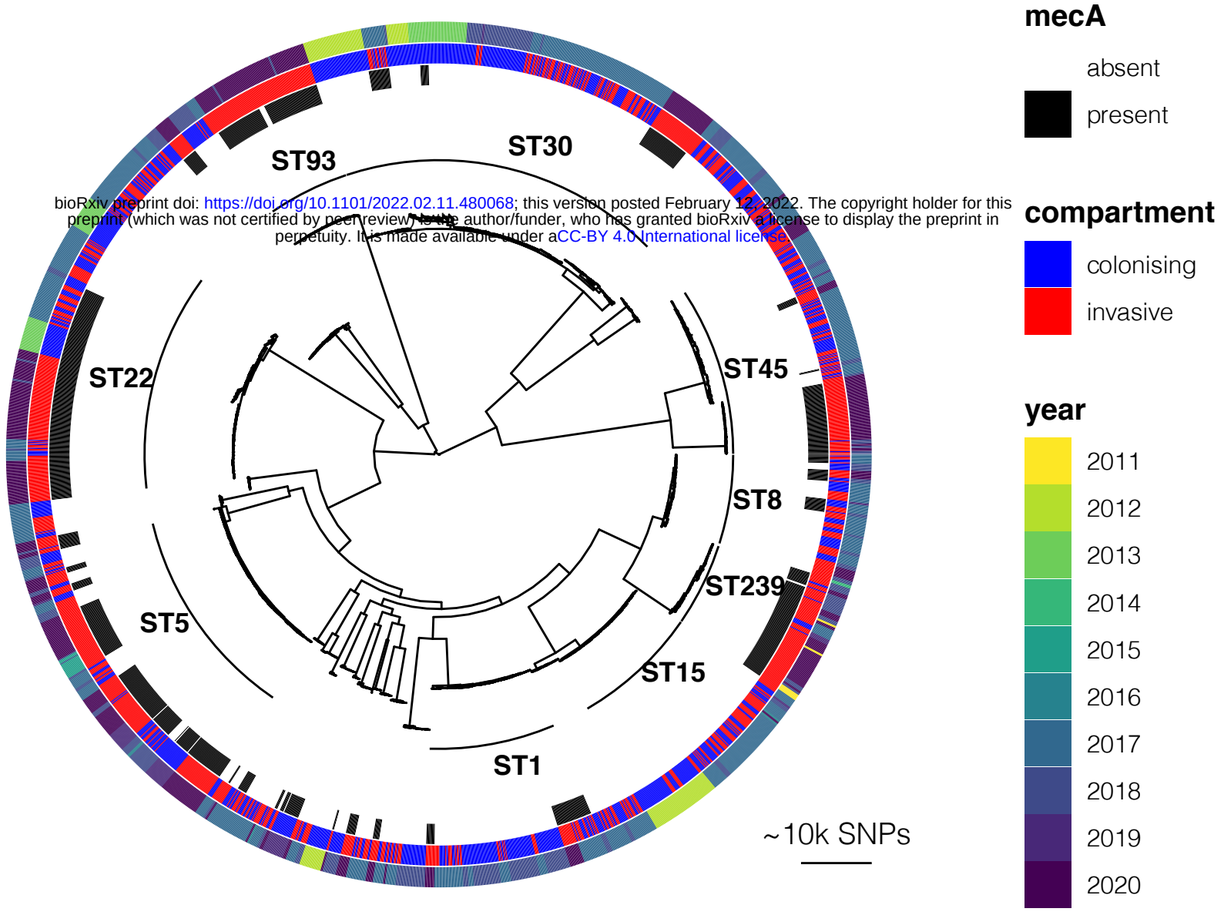

B

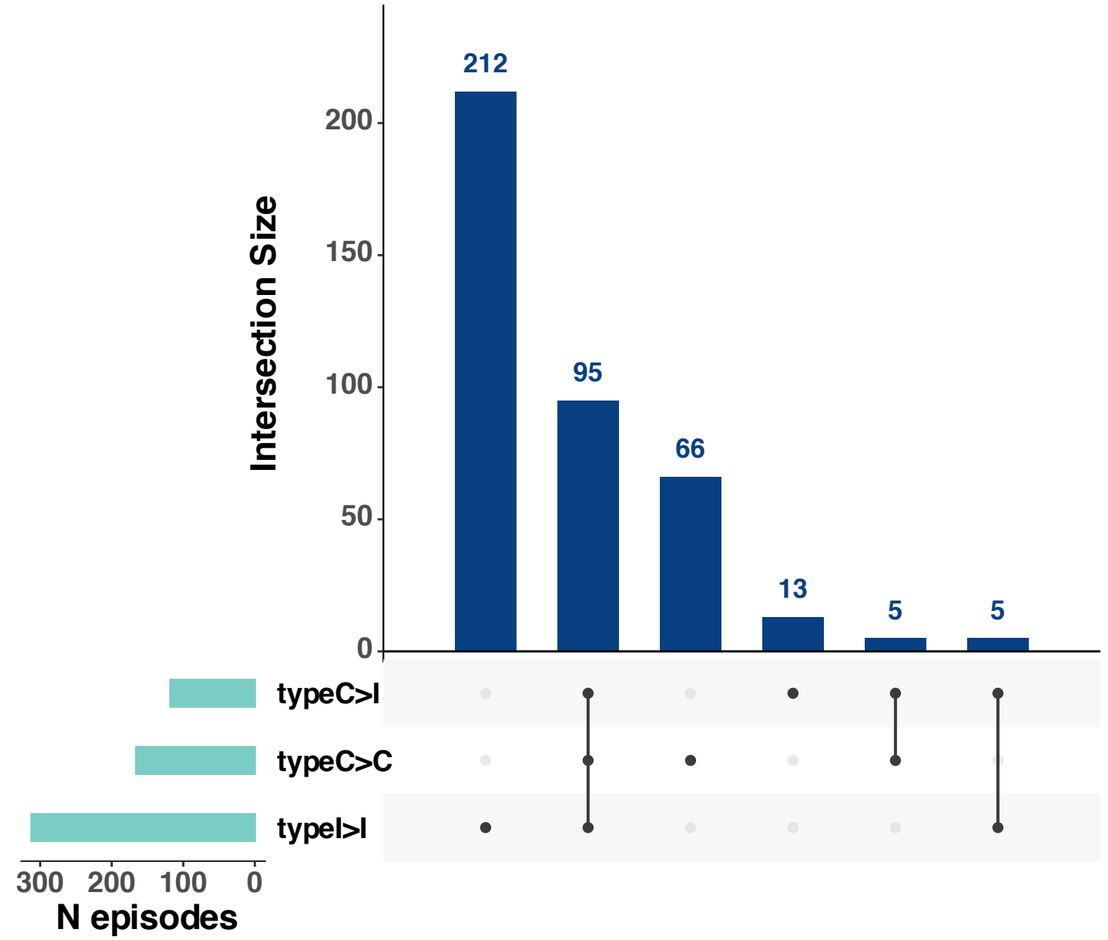

C

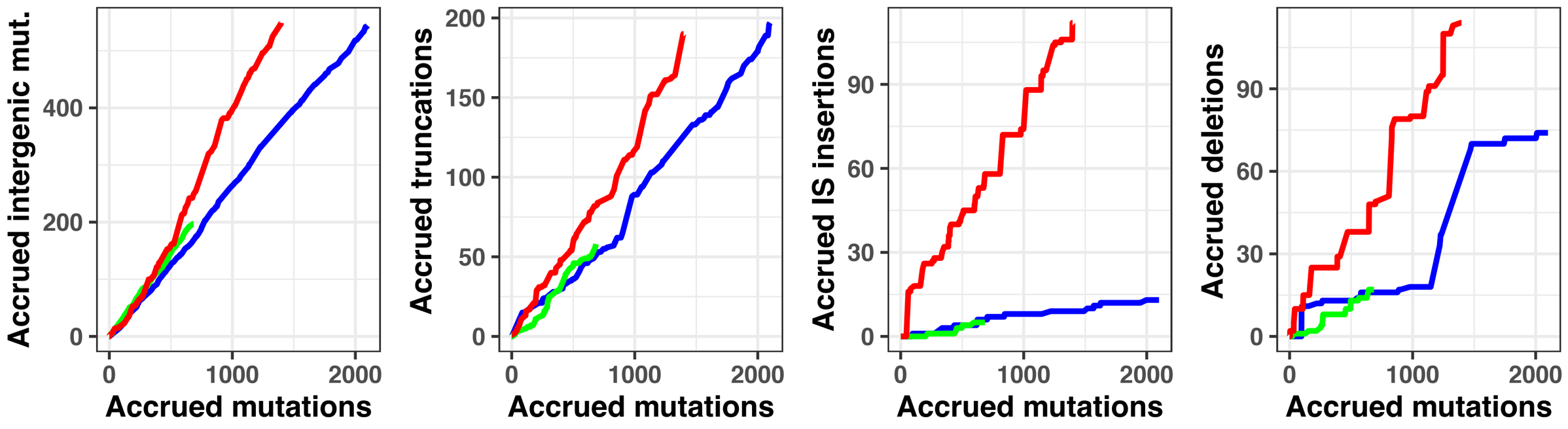

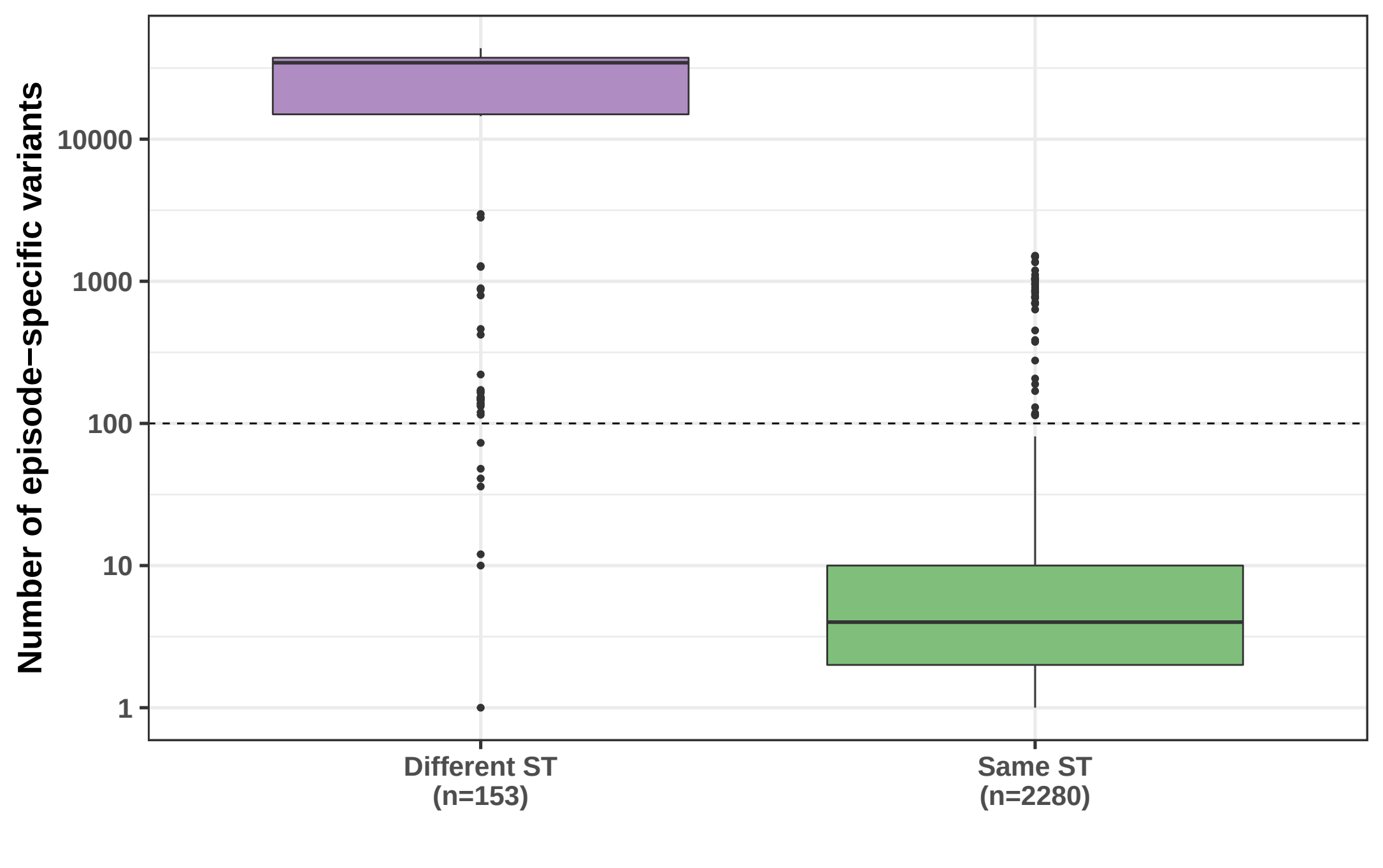
Number of episode−specific variants
10000
1000
100
10
1
Different ST
(n=153)
Same ST
(n=2280)

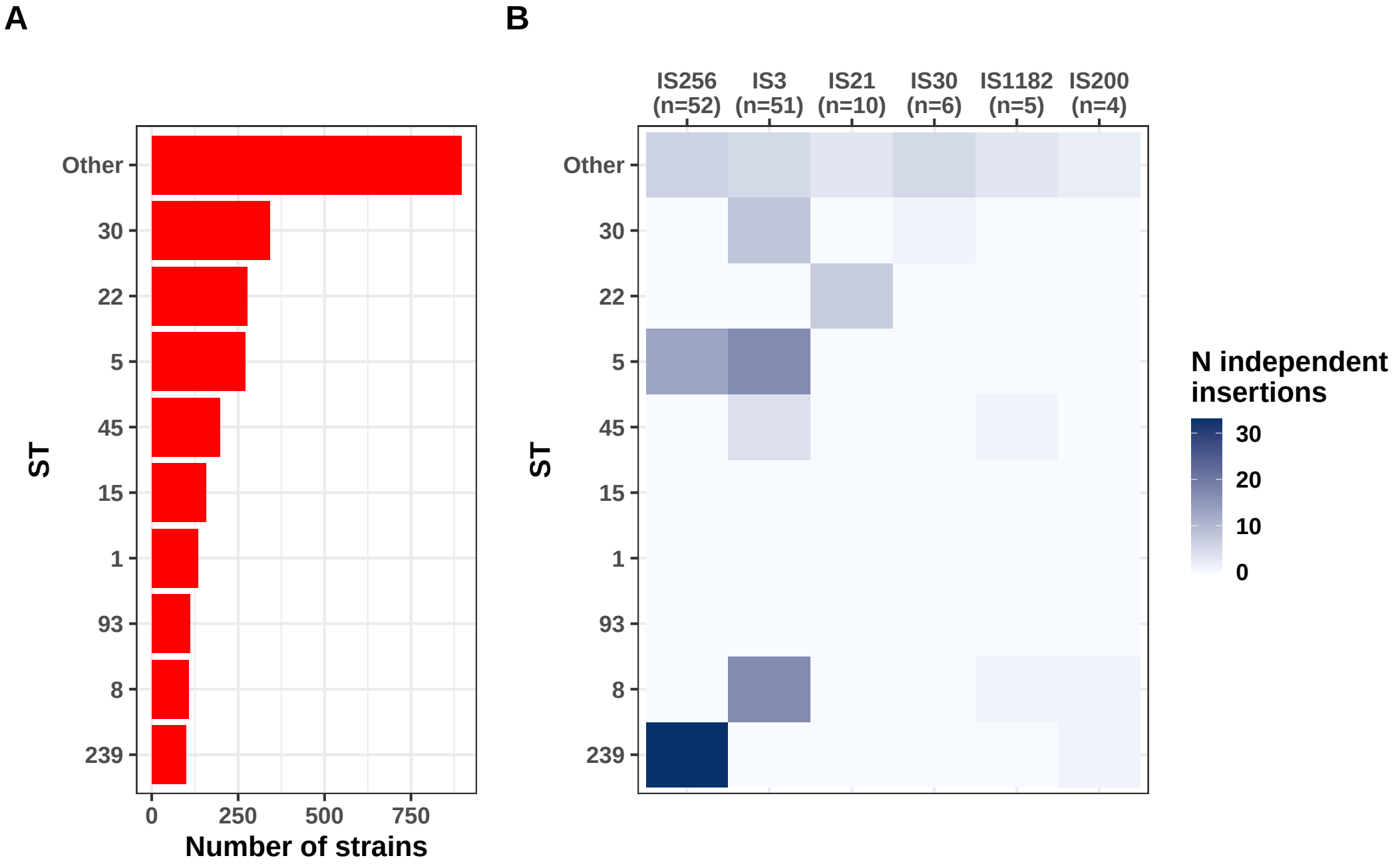
A
B
ST
Other
30
22
5
45
15
1
93
8
239
0
250
500
750
Number of strains
IS256 (n=52)
IS3 (n=51)
IS21 (n=10)
IS30 (n=6)
IS1182 (n=5)
IS200 (n=4)
N independent insertions
30
20
10
0

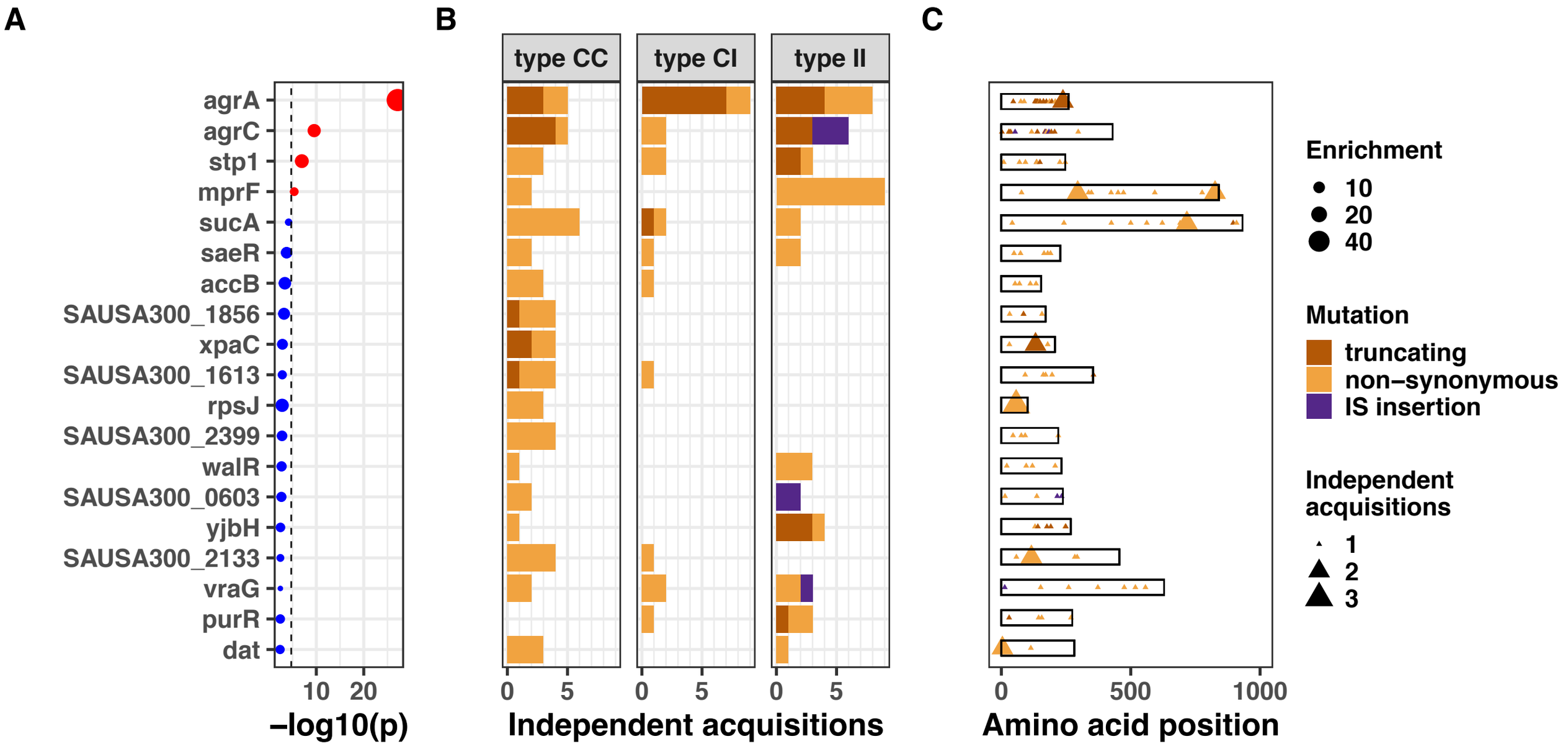
A
B
C
agrA
agrC
stp1
mprF
sucA
saeR
accB
SAUSA300_1856
xpaC
SAUSA300_1613
rpsJ
SAUSA300_2399
walR
SAUSA300_0603
yjbH
SAUSA300_2133
vraG
purR
dat
10
20
−log10(p)
type CC
type CI
type II
0
5
Independent acquisitions
0
500
1000
Amino acid position
Enrichment
10
20
40
Mutation
truncating
non−synonymous
IS insertion
Independent acquisitions
1
2
3

agrA

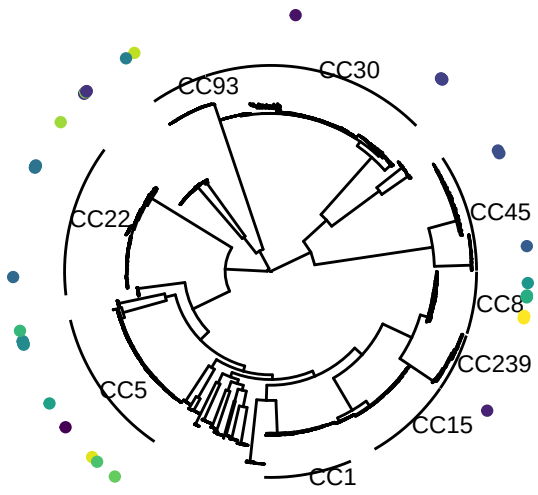

Mutation

- Q46*
- I75N
- T88M
- L131fs
- Ter133Lext*?
- D137fs
- Ter141fs
- G148D
- I150fs
- L162fs
- E163fs
- E163Y
- H174fs
- L186F
- F197fs
- R195C
- H208fs
- R218*
- R218C
- E226fs
- I238fs
- Y238fs

agrC

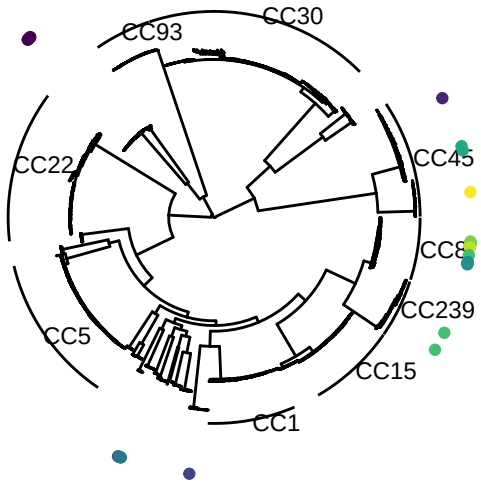

Mutation

- D2fs
- I30fs
- L38fs
- F117L
- F117LI139fs
- S28TI297V
- Y168fs
- IS insertion (intragenic)
- Q175E
- L193*
- K206fs

stp1

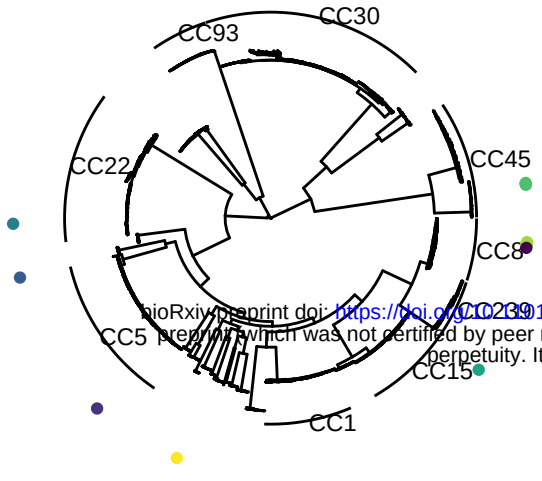

Mutation

- D9V
- Q70R
- N93_K111del
- S136fs
- N137D
- Q149*
- A226V
- V247L

mprF

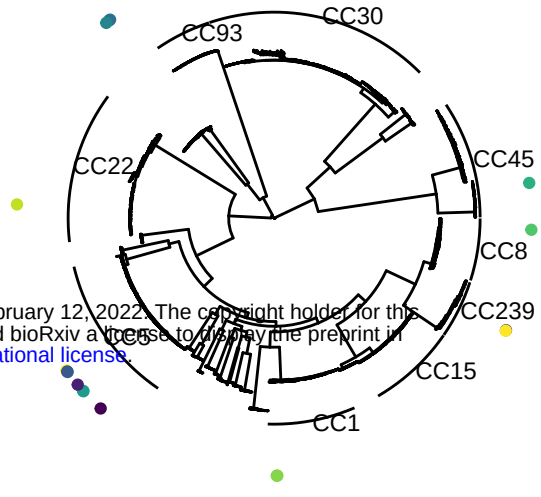

Mutation

- L78F
- S295A
- S295L
- P314L
- S337L
- I348del
- W424C
- L451_V452delinsF
- T472K
- E593D
- L776S
- L826F

sucA

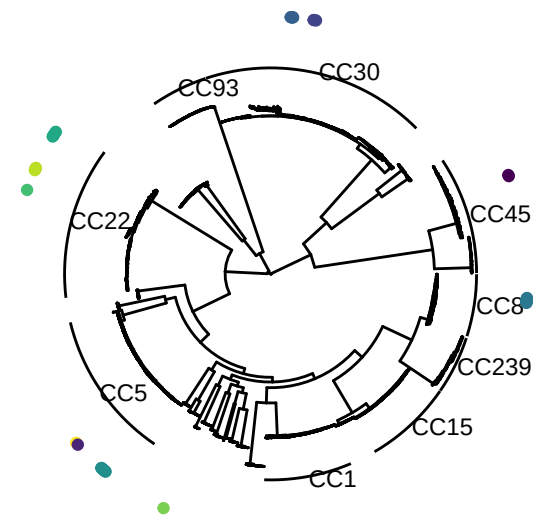

Mutation

- V42I
- H242Q
- V425D
- I500M
- P562T
- S622G
- S691P
- P717H
- P717T
- D897fs
- P909L

saeR

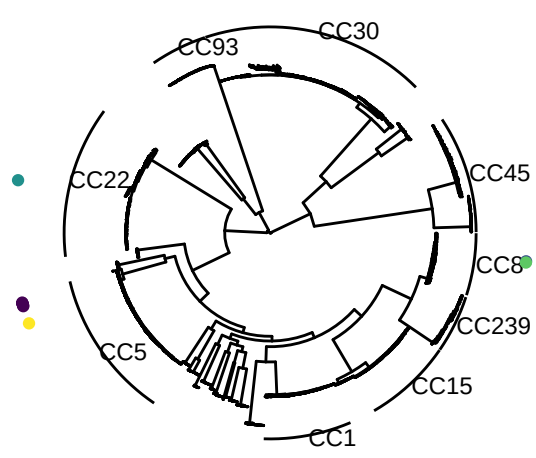

Mutation

- V49_M53del
- P74S
- A165D
- E179K
- A190T

accB

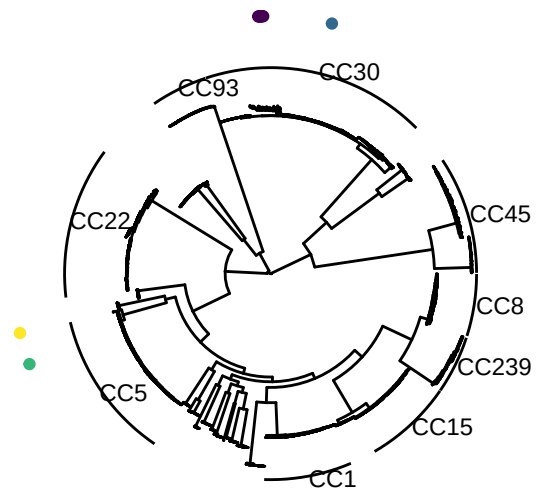

Mutation

- V53A
- A70T
- T112I
- I134V

SAUSA300_1856

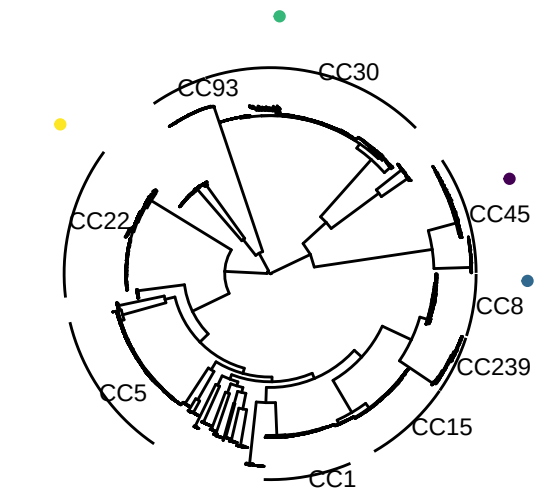

Mutation

- I32T
- G85A
- R86*
- D157Y

xpaC

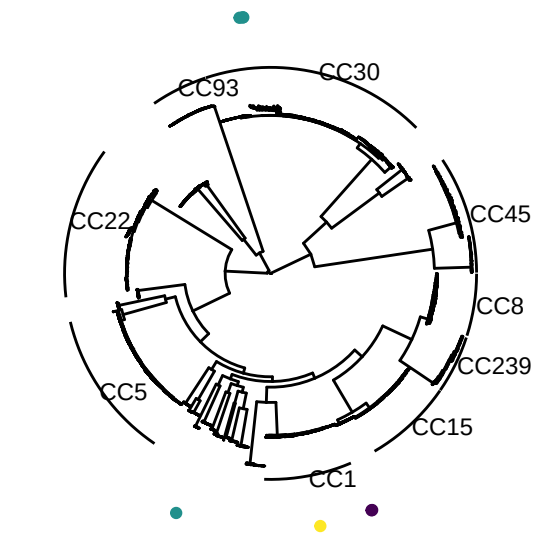

Mutation

- I31V
- Y132fs
- D179N

SAUSA300_1613

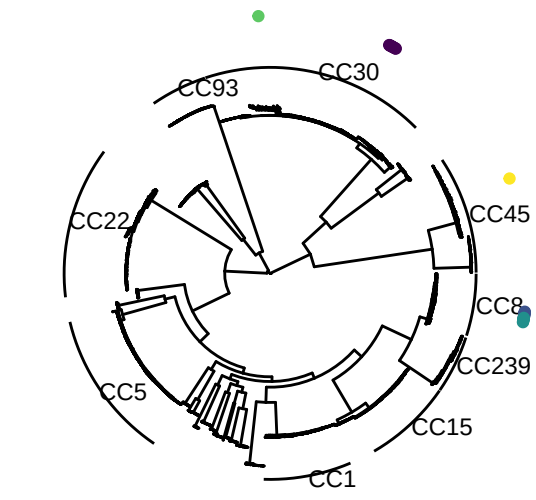

Mutation

- I92M
- L162F
- D171N
- I196T
- Ter356Yext*?

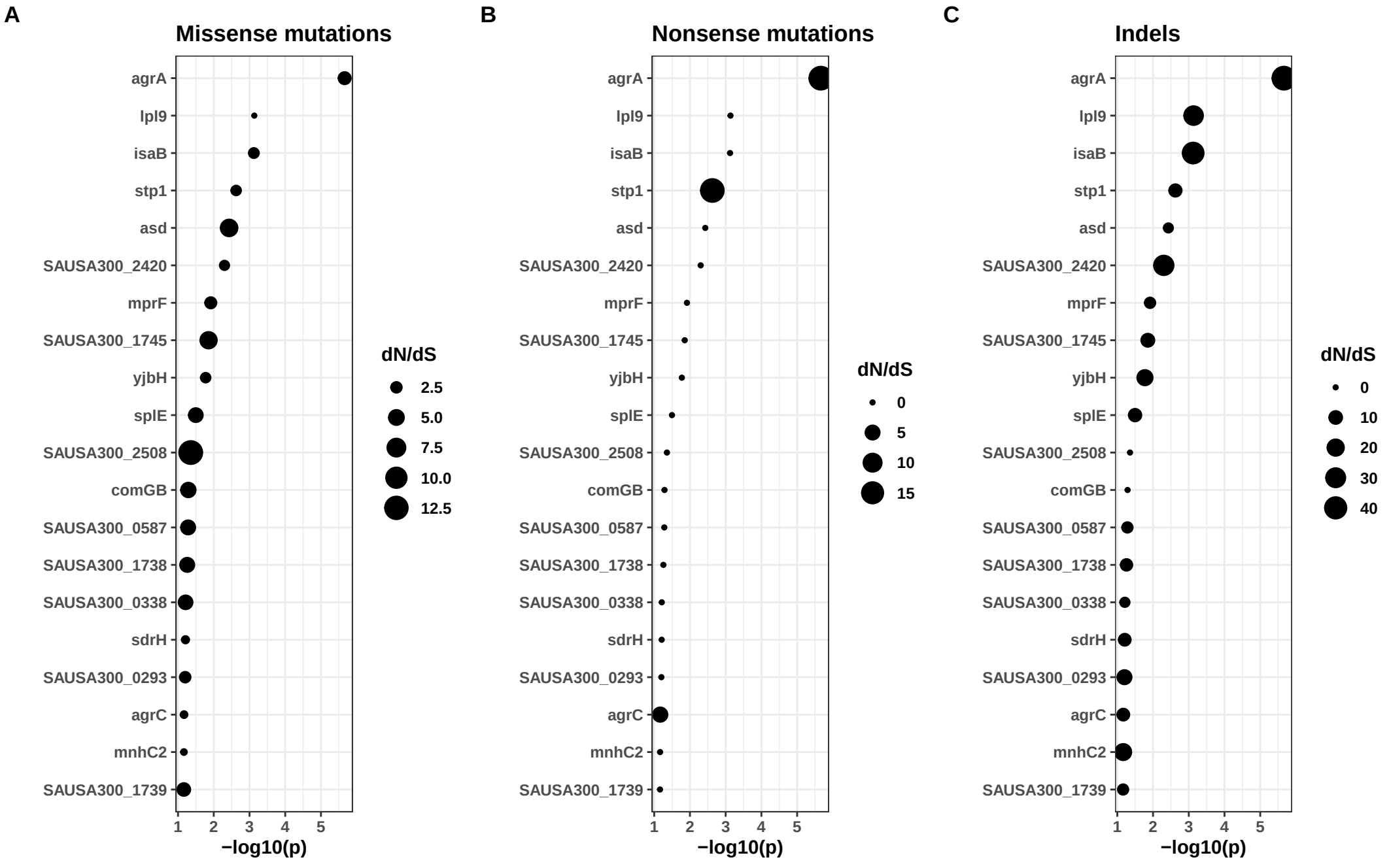
A
Missense mutations
B
Nonsense mutations
C
Indels
agrA
lpl9
isaB
stp1
asd
SAUSA300_2420
mprF
SAUSA300_1745
yjbH
splE
SAUSA300_2508
comGB
SAUSA300_0587
SAUSA300_1738
SAUSA300_0338
sdrH
SAUSA300_0293
agrC
mnhC2
SAUSA300_1739
1
2
3
4
5
−log10(p)
dN/dS
2.5
5.0
7.5
10.0
12.5
dN/dS
0
5
10
15
dN/dS
0
10
20
30
40

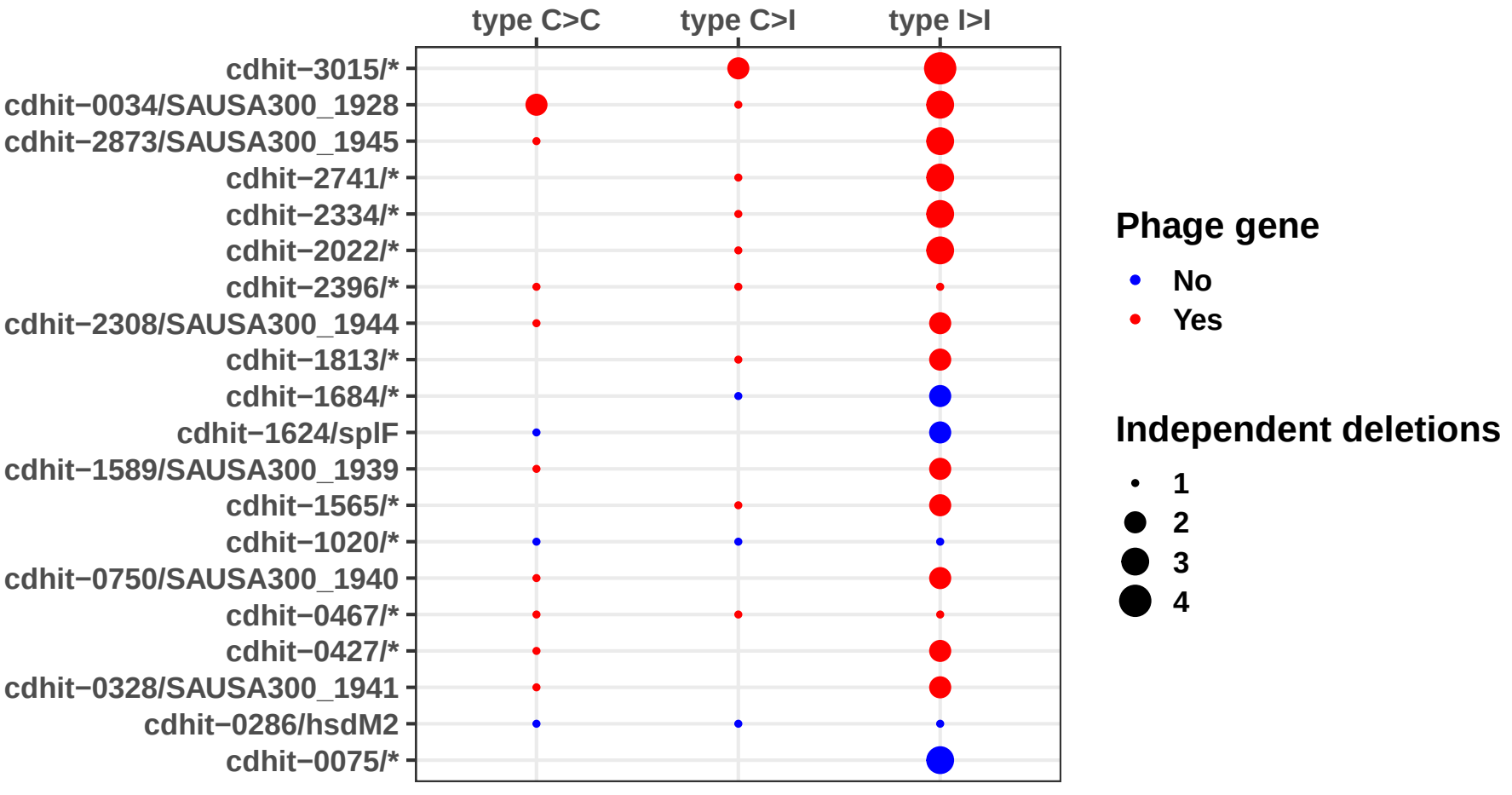
type C>C
type C>I
type I>I
cdhit−3015/*
cdhit−0034/SAUSA300_1928
cdhit−2873/SAUSA300_1945
cdhit−2741/*
cdhit−2334/*
cdhit−2022/*
cdhit−2396/*
cdhit−2308/SAUSA300_1944
cdhit−1813/*
cdhit−1684/*
cdhit−1624/splF
cdhit−1589/SAUSA300_1939
cdhit−1565/*
cdhit−1020/*
cdhit−0750/SAUSA300_1940
cdhit−0467/*
cdhit−0427/*
cdhit−0328/SAUSA300_1941
cdhit−0286/hsdM2
cdhit−0075/*
Phage gene
No
Yes
Independent deletions
1
2
3
4

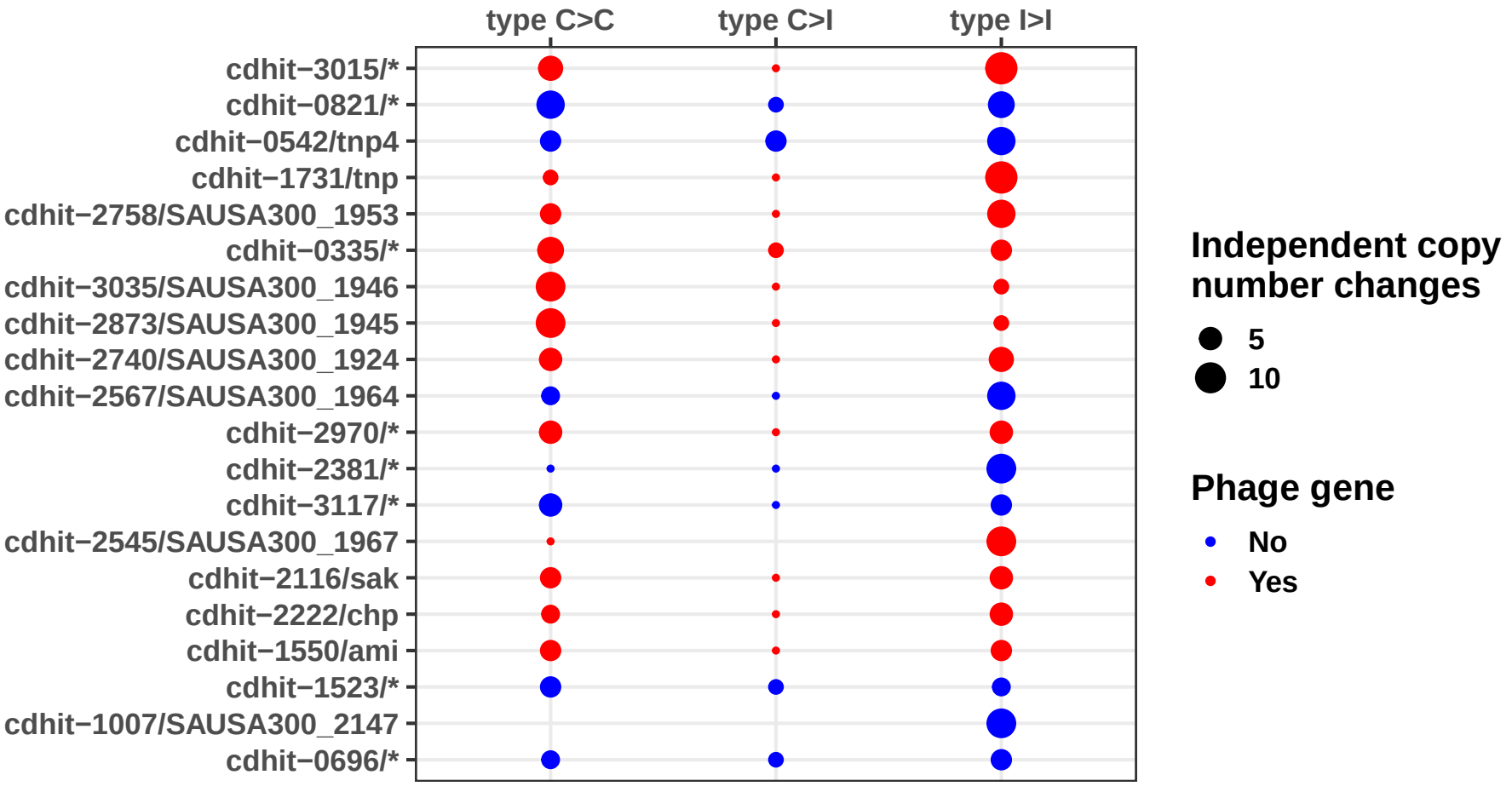
type C>C
type C>I
type I>I
cdhit−3015/*
cdhit−0821/*
cdhit−0542/tnp4
cdhit−1731/tnp
cdhit−2758/SAUSA300_1953
cdhit−0335/*
cdhit−3035/SAUSA300_1946
cdhit−2873/SAUSA300_1945
cdhit−2740/SAUSA300_1924
cdhit−2567/SAUSA300_1964
cdhit−2970/*
cdhit−2381/*
cdhit−3117/*
cdhit−2545/SAUSA300_1967
cdhit−2116/sak
cdhit−2222/chp
cdhit−1550/ami
cdhit−1523/*
cdhit−1007/SAUSA300_2147
cdhit−0696/*
Independent copy number changes
5
10
Phage gene
No
Yes

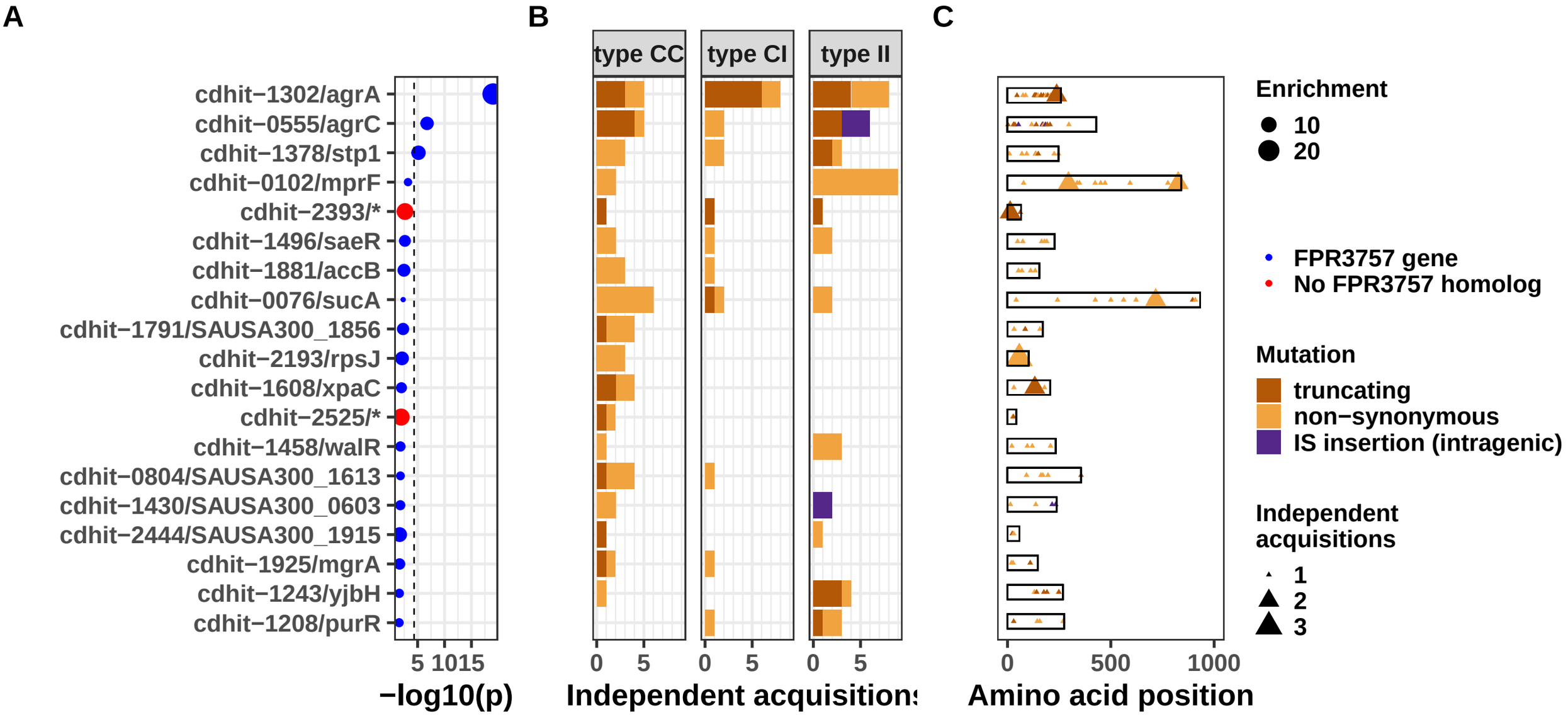
A
B
C
cdhit−1302/agrA
cdhit−0555/agrC
cdhit−1378/stp1
cdhit−0102/mprF
cdhit−2393/*
cdhit−1496/saeR
cdhit−1881/accB
cdhit−0076/sucA
cdhit−1791/SAUSA300_1856
cdhit−2193/rpsJ
cdhit−1608/xpaC
cdhit−2525/*
cdhit−1458/walR
cdhit−0804/SAUSA300_1613
cdhit−1430/SAUSA300_0603
cdhit−2444/SAUSA300_1915
cdhit−1925/mgrA
cdhit−1243/yjbH
cdhit−1208/purR
5 1015
−log10(p)
type CC
type CI
type II
0 5
0 5
0 5
Independent acquisitions
0
500
1000
Amino acid position
Enrichment
10
20
FPR3757 gene
No FPR3757 homolog
Mutation
truncating
non−synonymous
IS insertion (intragenic)
Independent acquisitions
1
2
3

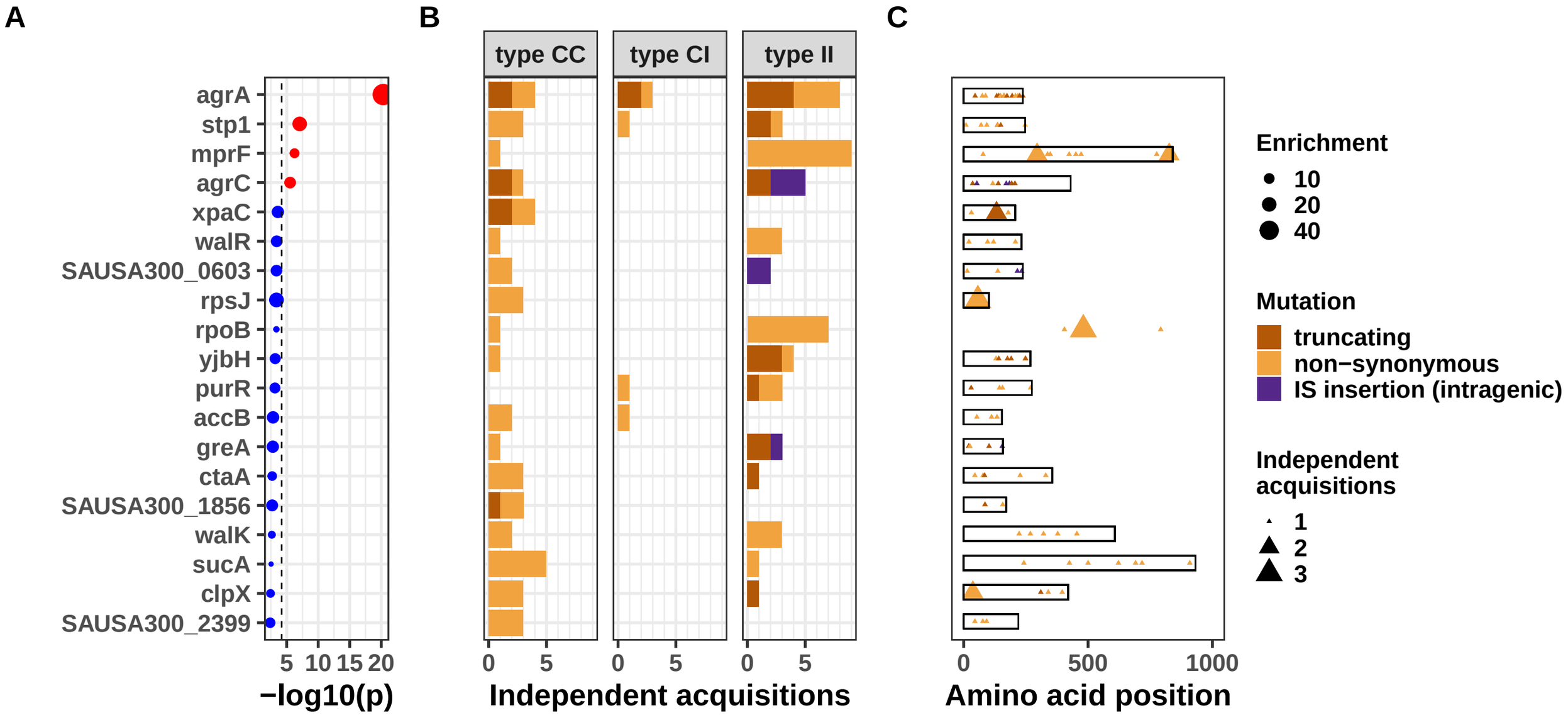
A
agrA
stp1
mprF
agrC
xpaC
walR
SAUSA300_0603
rpsJ
rpoB
yjbH
purR
accB
greA
ctaA
SAUSA300_1856
walK
sucA
clpX
SAUSA300_2399
5 10 15 20
−log10(p)
B
type CC
type CI
type II
0 5
0 5
0 5
Independent acquisitions
C
0 500 1000
Amino acid position
Enrichment
10
20
40
Mutation
truncating
non−synonymous
IS insertion (intragenic)
Independent acquisitions
1
2
3

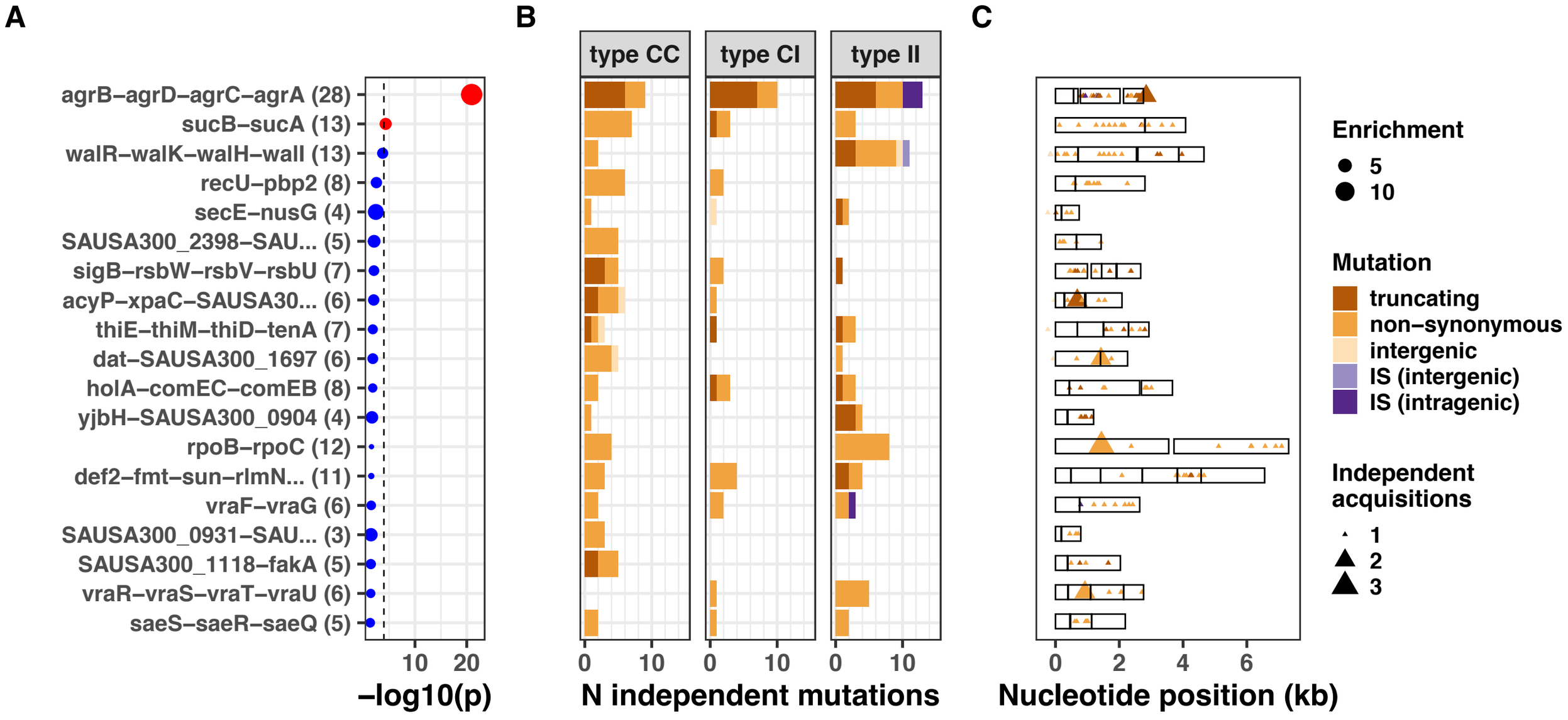
A
agrB–agrD–agrC–agrA (28)
sucB–sucA (13)
walR–walK–walH–walI (13)
recU–pbp2 (8)
secE–nusG (4)
SAUSA300_2398–SAU... (5)
sigB–rsbW–rsbV–rsbU (7)
acyP–xpaC–SAUSA30... (6)
thiE–thiM–thiD–tenA (7)
dat–SAUSA300_1697 (6)
holA–comEC–comEB (8)
yjbH–SAUSA300_0904 (4)
rpoB–rpoC (12)
def2–fmt–sun–rlmN... (11)
vraF–vraG (6)
SAUSA300_0931–SAU... (3)
SAUSA300_1118–fakA (5)
vraR–vraS–vraT–vraU (6)
saeS–saeR–saeQ (5)
10
20
–log10(p)
B
type CC
type CI
type II
0
10
0
10
0
10
N independent mutations
C
0
2
4
6
Nucleotide position (kb)
Enrichment
5
10
Mutation
truncating
non–synonymous
intergenic
IS (intergenic)
IS (intragenic)
Independent acquisitions
1
2
3

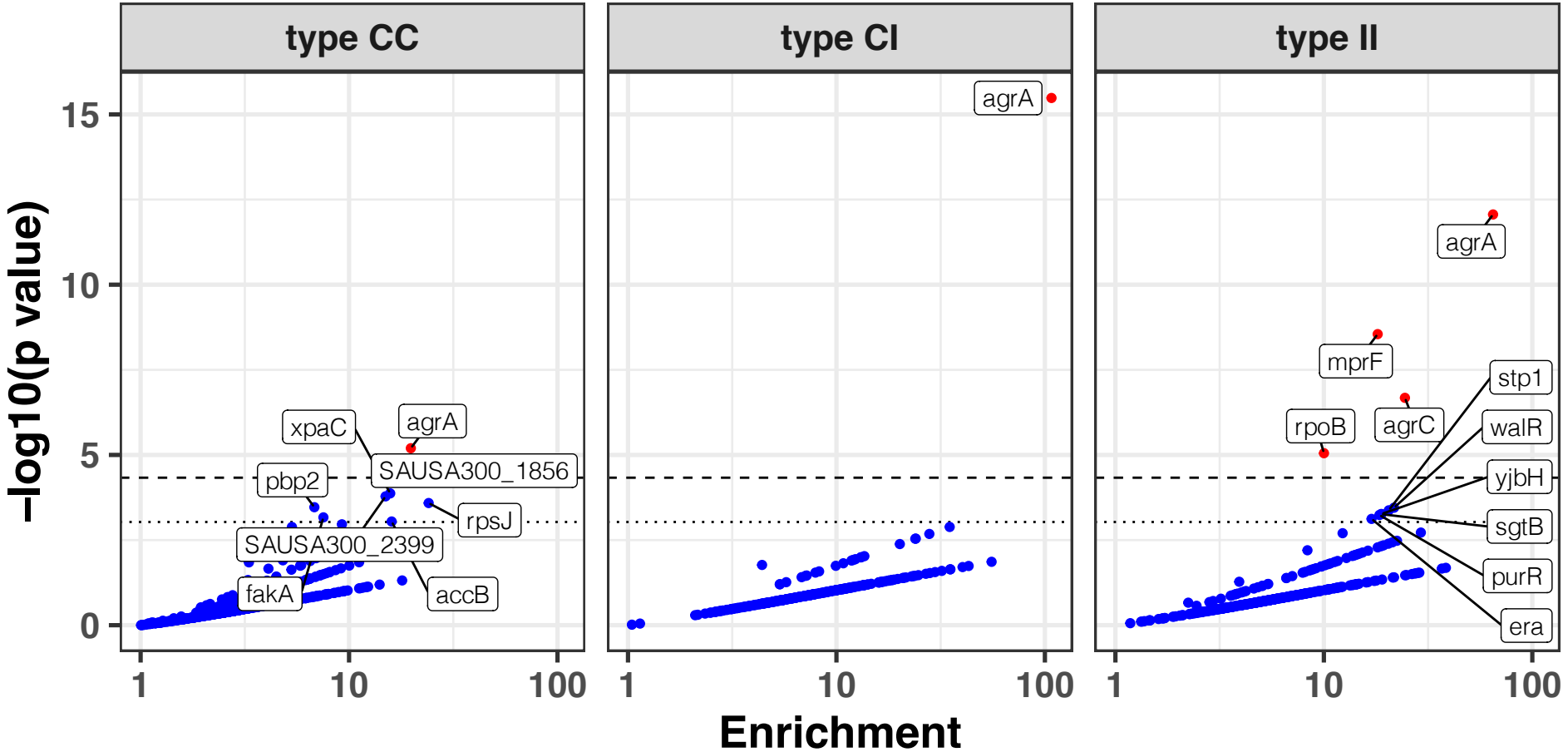
type CC
type CI
type II
−log10(p value)
15
10
5
0
1
10
100
Enrichment
xpaC
agrA
pbp2
SAUSA300_1856
rpsJ
SAUSA300_2399
fakA
accB
agrA
agrA
mprF
stp1
rpoB
agrC
walR
yjbH
sgtB
purR
era

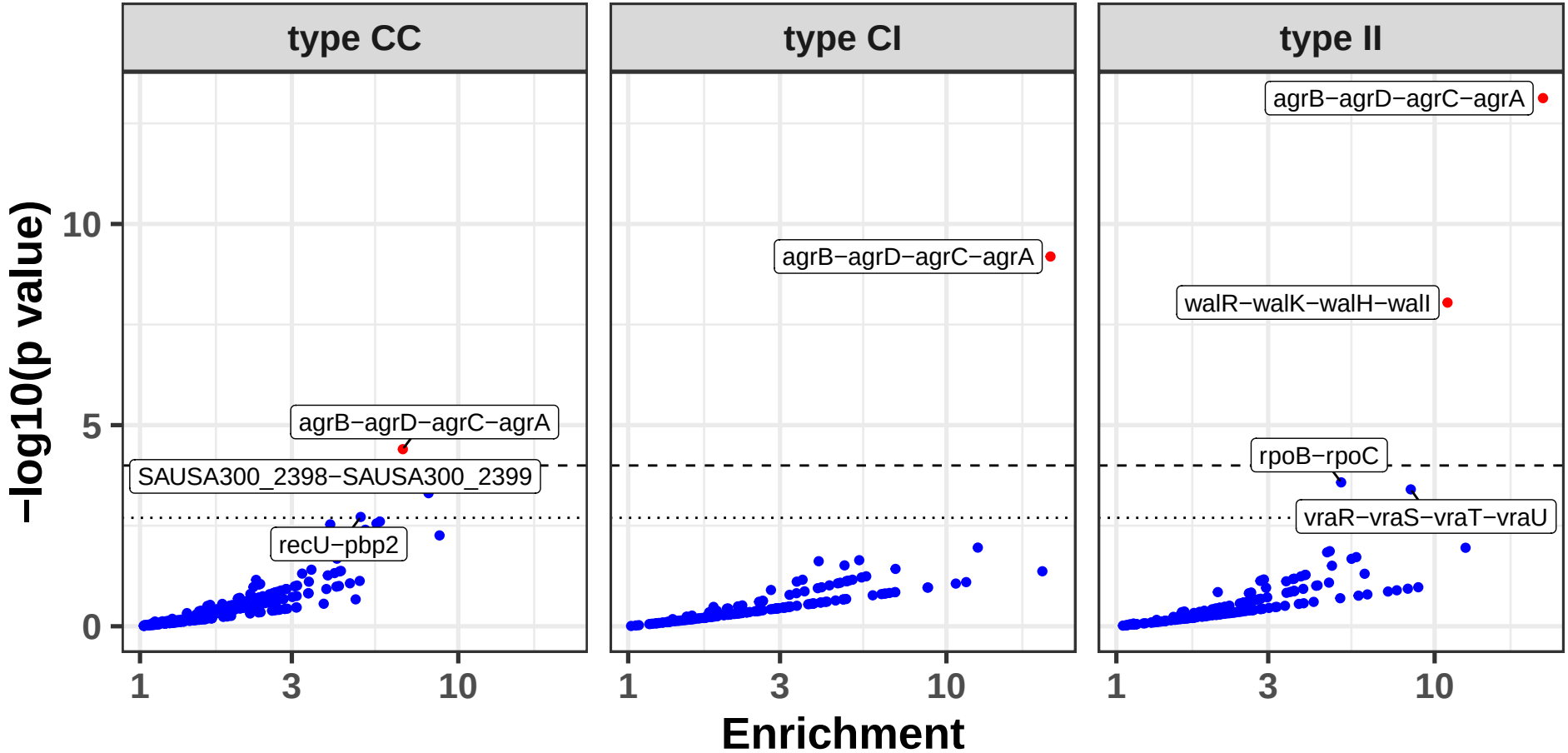
type CC
type CI
type II
−log10(p value)
10
5
0
1
3
10
Enrichment
agrB−agrD−agrC−agrA
SAUSA300_2398−SAUSA300_2399
recU−pbp2
agrB−agrD−agrC−agrA
agrB−agrD−agrC−agrA
walR−walK−walH−walI
rpoB−rpoC
vraR−vraS−vraT−vraU

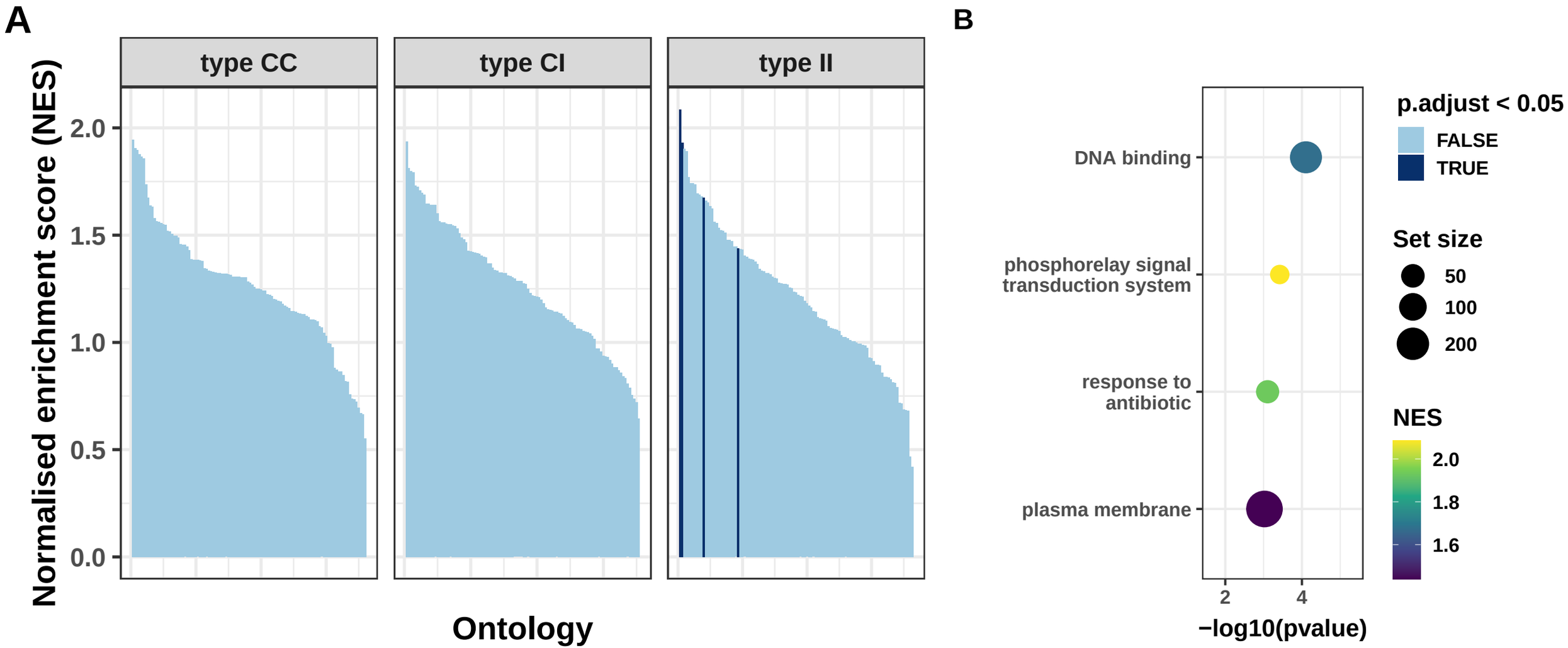
A
type CC
type CI
type II
Normalised enrichment score (NES)
2.0
1.5
1.0
0.5
0.0
Ontology
B
DNA binding
phosphorelay signal transduction system
response to antibiotic
plasma membrane
2
4
−log10(pvalue)
p.adjust < 0.05
FALSE
TRUE
Set size
50
100
200
NES
2.0
1.8
1.6

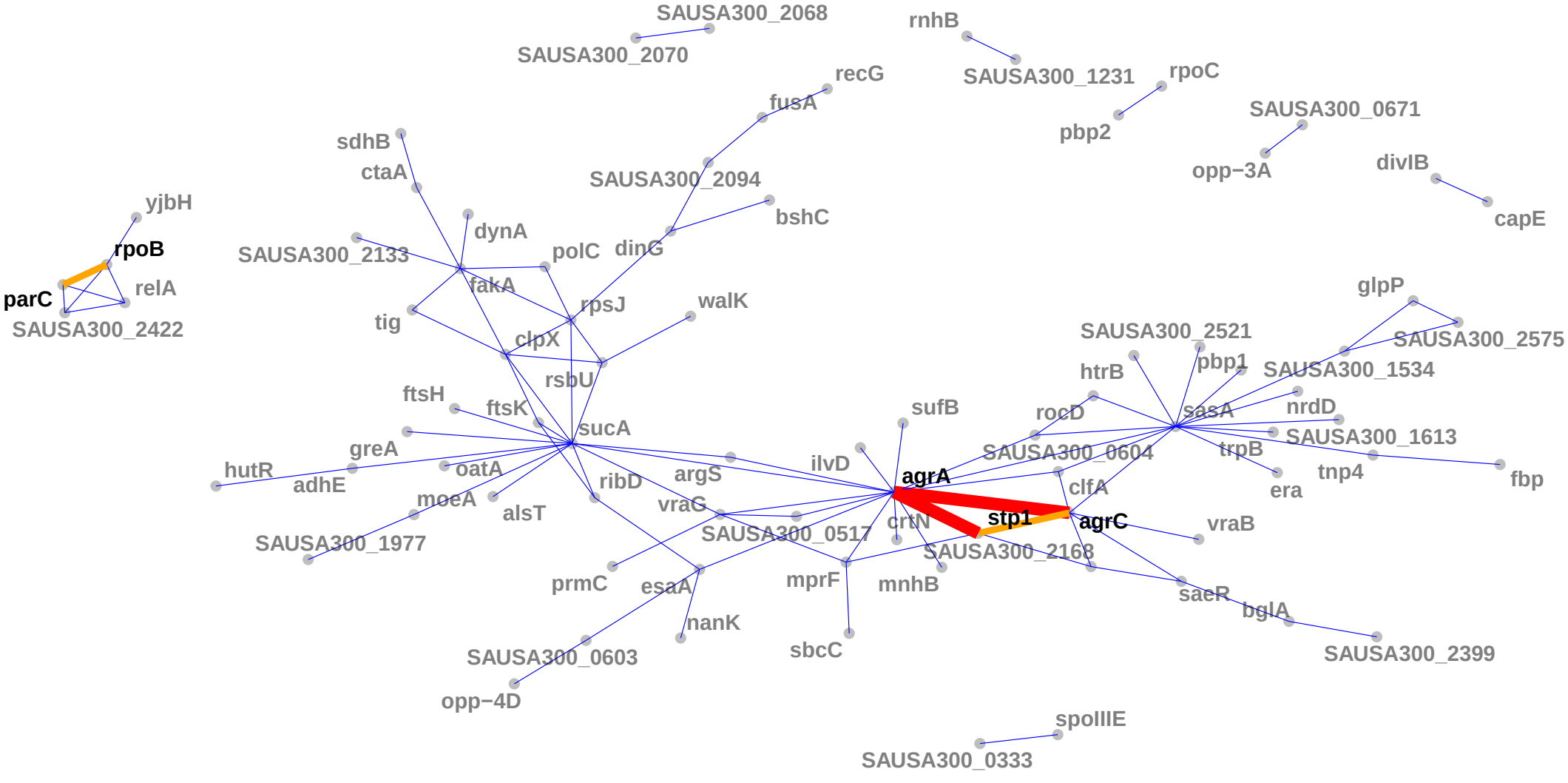
SAUSA300_2068
SAUSA300_2070
rnhB
SAUSA300_1231
rpoC
pbp2
SAUSA300_0671
opp−3A
divIB
capE
recG
fusA
sdhB
ctaA
SAUSA300_2094
bshC
yjbH
rpoB
parC
relA
SAUSA300_2422
dynA
SAUSA300_2133
polC
dinG
fakA
tig
rpsJ
walK
clpX
rsbU
glpP
SAUSA300_2521
SAUSA300_2575
htrB
pbp1
SAUSA300_1534
ftsH
ftsK
sucA
sufB
rocD
sasA
nrdD
SAUSA300_1613
greA
hutR
adhE
oatA
ilvD
SAUSA300_0604
trpB
tnp4
fbp
era
agrA
clfA
ribD
argS
moeA
alsT
vraG
crtN
stp1
agrC
vraB
SAUSA300_1977
SAUSA300_0517
SAUSA300_2168
prmC
esaA
mprF
mnhB
saeR
bglA
nanK
sbcC
SAUSA300_2399
SAUSA300_0603
opp−4D
spoIIIE
SAUSA300_0333

A

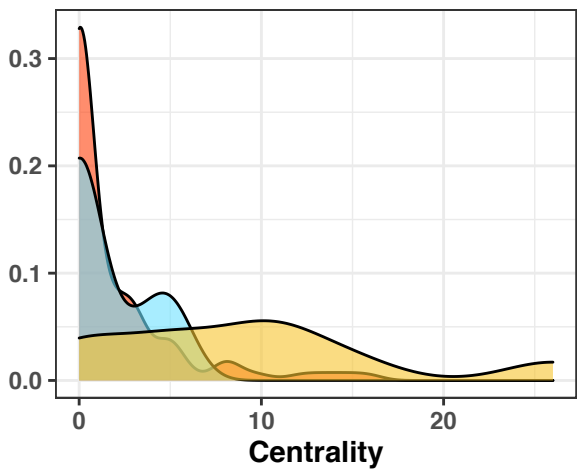

B

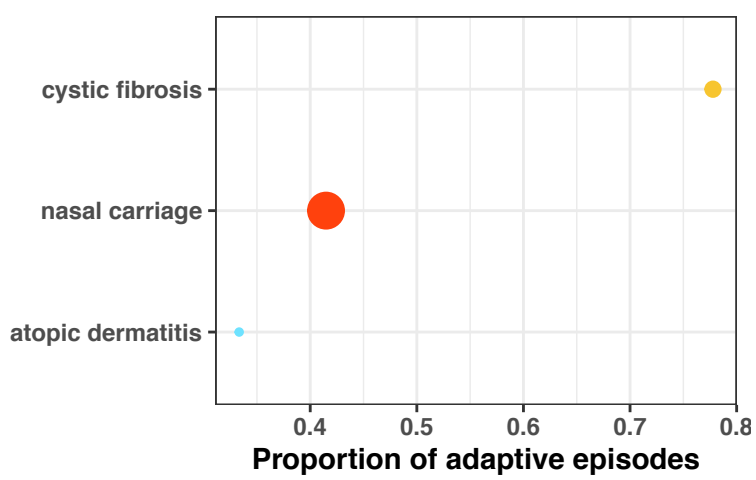

C

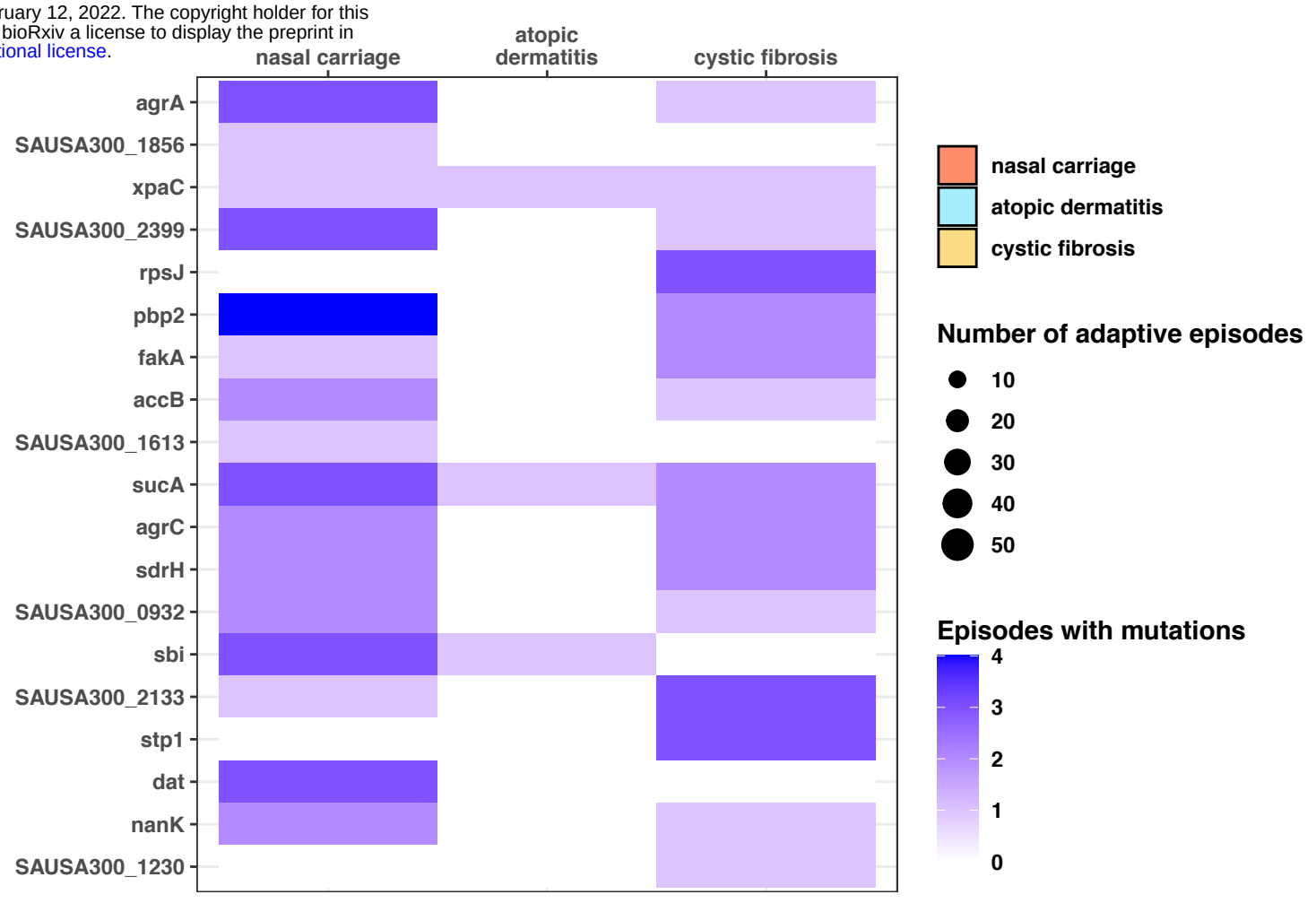

D

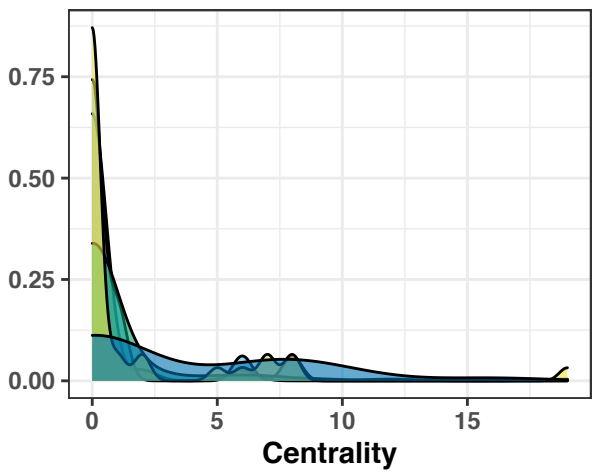

E

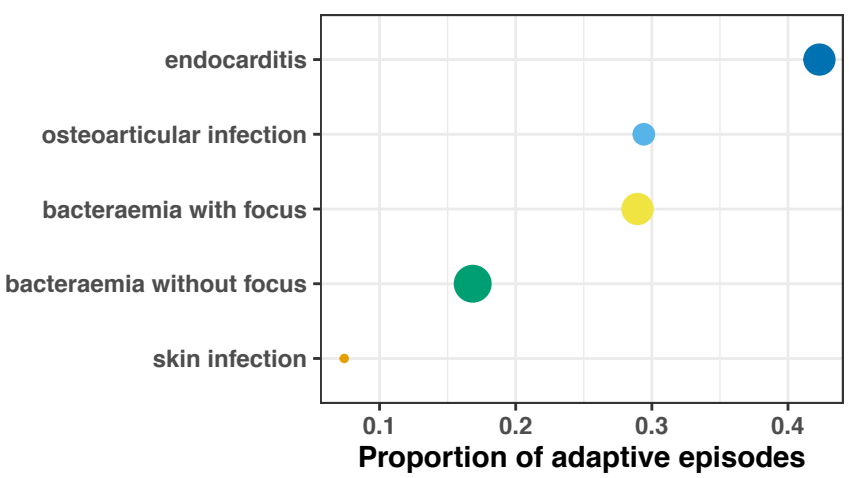

F

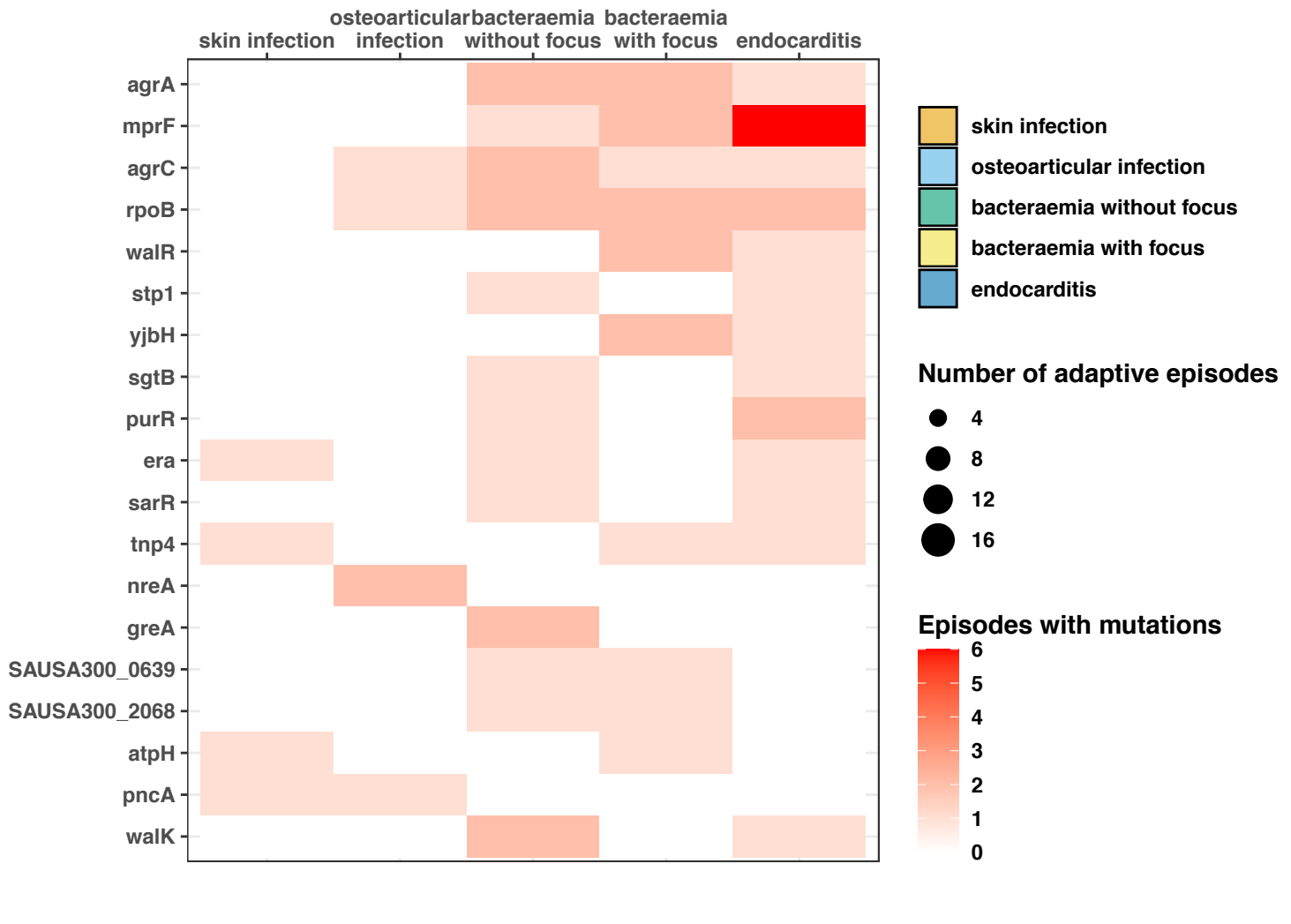

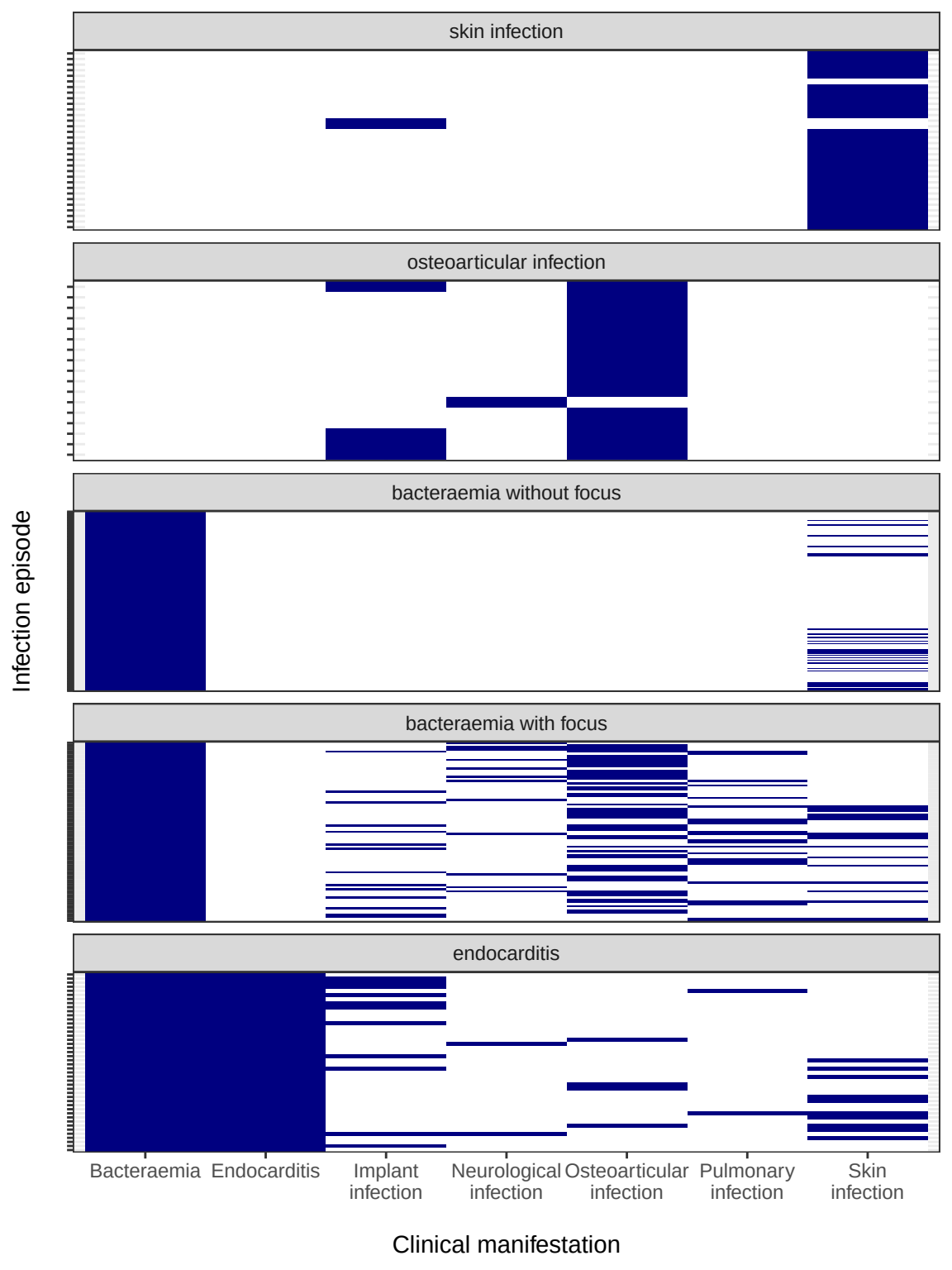
skin infection
osteoarticular infection
bacteraemia without focus
bacteraemia with focus
endocarditis
Infection episode
Bacteraemia
Endocarditis
Implant infection
Neurological infection
Osteoarticular infection
Pulmonary infection
Skin infection
Clinical manifestation

Adaption network of type II variants

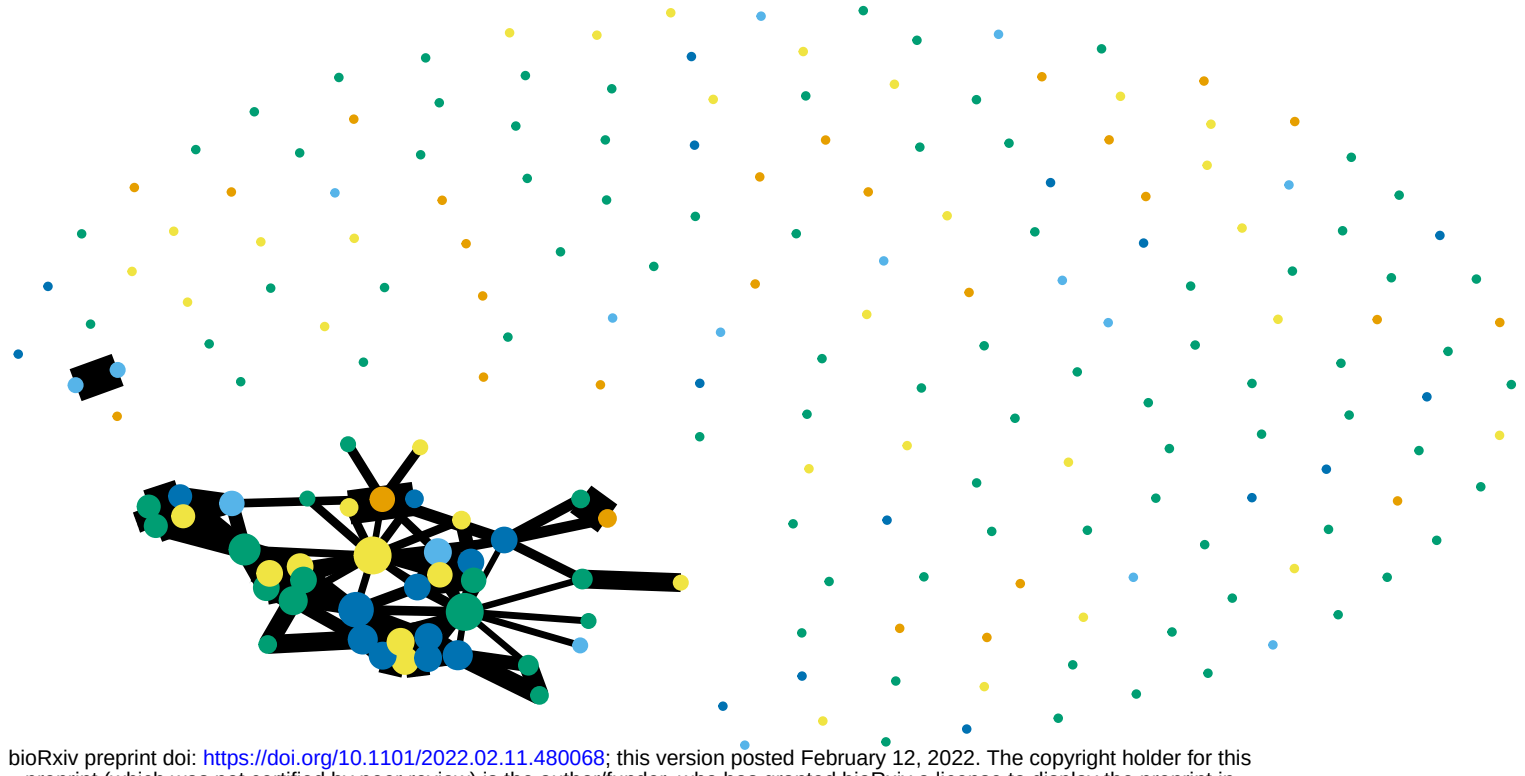

Adaptation network of type CC variants

Adaptation network of type CI variants